

Shining light on the antenna chromophore in lanthanide based dyes

Anne Kathrine R. Junker,^a Leila R. Hill,^b Amber L. Thompson,^b Stephen Faulkner*^b and Thomas Just Sørensen*^a

Contents

Contents.....	1
Single Crystal X-ray Diffraction Studies	2
NMR spectra of synthesised compounds.....	7
Optical Spectroscopy:.....	14
Absorption Spectra	14
Excitation Spectra	16
Emission Spectra.....	19
Phosphorescence spectra.....	21
Quantum Yield determination.....	25
Fluorescence & Luminescence Lifetime decays and fits.....	29

Single Crystal X-ray Diffraction Studies

Multiple attempts were made to determine the structure of **Eu.L** using low temperature single crystal X-ray diffraction. Initially attempts were made to collect data at 150 K using a (Rigaku) Oxford Diffraction Supernova in-house diffractometer ($\lambda = 1.54184 \text{ \AA}$) fitted with an Oxford Cryosystem 700 Series Cryostream.¹ The data were poor (Figure S1), but indexed to give a monoclinic cell of $52.639(8) \text{ \AA}$, $18.0664(15) \text{ \AA}$, $32.737(3) \text{ \AA}$, $\beta = 106.707(19)^\circ$. Data were initially collected just to investigate the connectivity, as the unit cell was much larger than originally expected for this material. The structure solved with Superflip² to give a structure in the monoclinic space group P2/c with two **Eu.L** tetramers in the asymmetric unit.

The raw data were of poor quality, so the sample was taken to beamline I19-1³ at Diamond Light Source where data were collected at 100 K ($\lambda = 0.6889 \text{ \AA}$). Although the crystals scattered slightly better at the start, they quickly suffered radiation damage which led to peak splitting and broadening as well as a loss of resolution (Figure S2). The data indexed, however, this time giving a triclinic cell of $17.33(3) \text{ \AA}$, $25.50(5) \text{ \AA}$, $33.32(5) \text{ \AA}$, $\alpha = 105.59(16)^\circ$, $\beta = 90.48(14)^\circ$, $\gamma = 103.20(19)^\circ$.

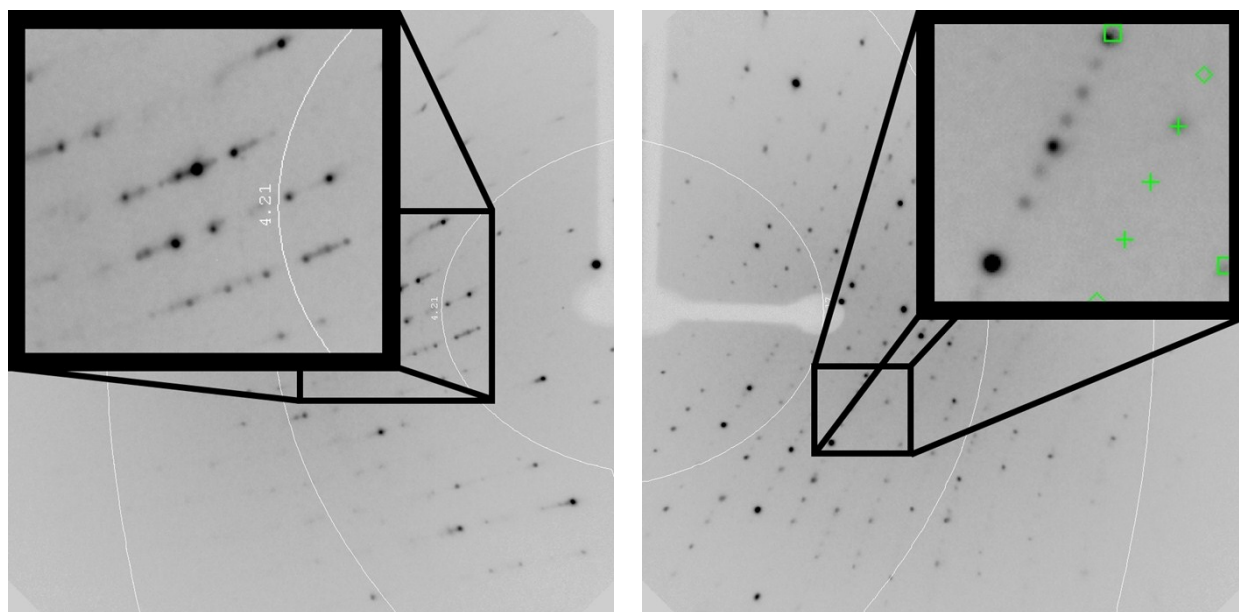


Figure S1. Two 1° images collected using an (Rigaku) Oxford Diffraction Supernova in-house diffractometer. The diffuse scattering between reflections (left) and additional weak reflections (right) suggestive of modulation are both visible.

¹ J. Cosier & A. M. Glazer, 1986, *J. Appl. Cryst.*, 19, 105-107.

² L. Palatinus, and G. Chapuis, 2007, *J. Appl. Cryst.*, 40, 786-790.

³ D. R Allan, H. Nowell, S. A. Barnett, M. R. Warren, A. Wilcox, J. Christensen, L. K. Saunders, A. Peach, M. T. Hooper, L. Zaja, S. Patel, L. Cahill, R. Mashall, S. Trimnell, A. J. Foster, T. Bates, S. Lay, M. A. Williams P. V. Hathaway, G. Winter, M. Gerstel and R. W. Wooley, *Crystals*, manuscript submitted.

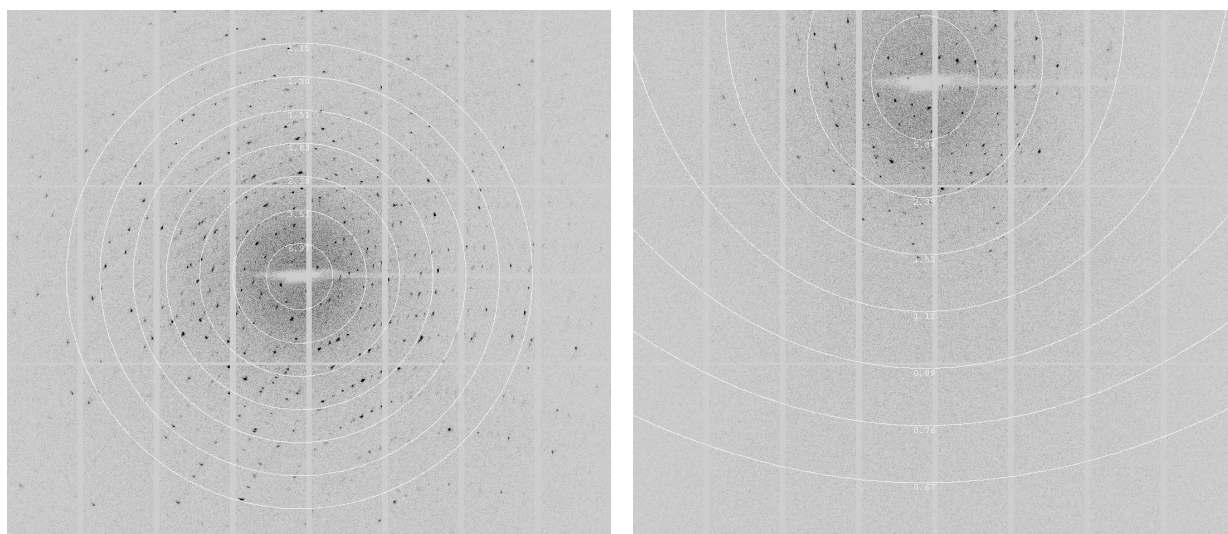


Figure S2. Two 0.2° images collected using beamline I19-1 at Diamond Light Source fitted with a Pilatus 2M photon counting detector. The first image (left) shows diffraction at or beyond atomic resolution (1 \AA) however, that quickly disappears as the radiation damage takes effect and there is barely any data beyond 2.5 \AA (right).

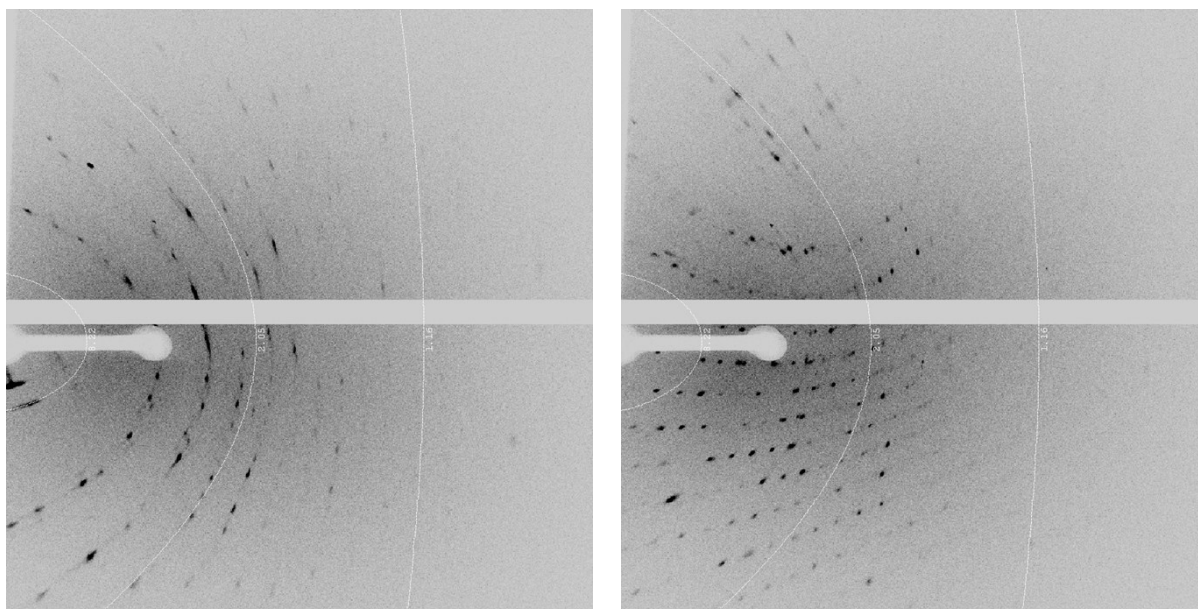


Figure S3. Two 0.15° images collected using a Rigaku Oxford Diffraction XtaLAB Synergy with HyPix detector showing the poor shape of the reflections and the lack of high resolution data.

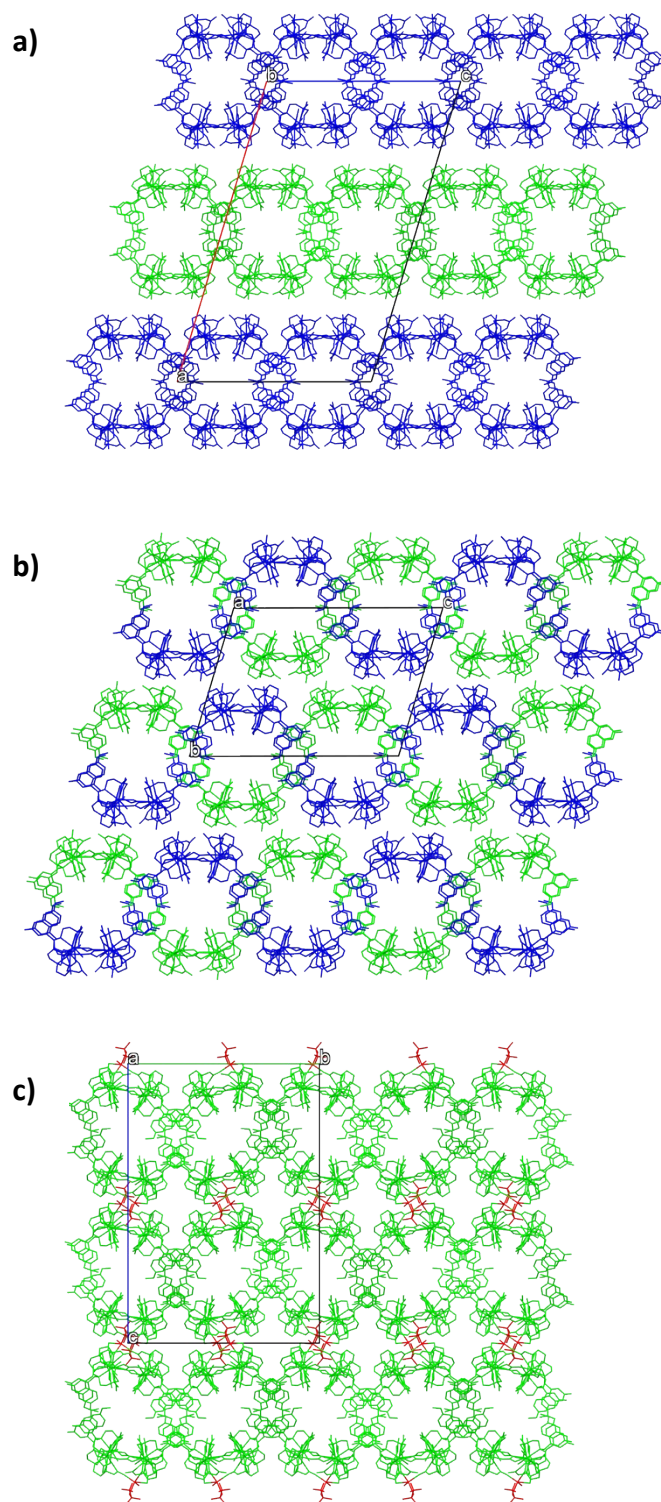


Figure S4. Crystal packing for the three polymorphs/solvates: monoclinic (a), triclinic (b) and orthorhombic (c), with the hydrogen atoms omitted for clarity. The symmetry equivalents are shown in blue and green and the NaOTf.H₂O is shown in red for the orthorhombic form (where it was modelled). All three structures consist of layers, but in a) and b) the layers are translated parallel to the c-axis.

These data were processed using Xia2⁴ and solved in P1 using ShelXT,⁵ again giving a structure with two **Eu.L** tetramers in the asymmetric unit.

An opportunity arose to collect data at Rigaku Oxford Diffraction's demonstration facility in Culham using their new XtaLAB Synergy with HyPix detector ($\lambda = 1.54184 \text{ \AA}$). Although the sample had already been severely plundered, there were a few crystals left. It was clear that these crystals had suffered over time, but a crystal was found that indexed, this time with an orthorhombic cell of 17.809(6) \AA , 32.896(8) \AA , 48.07(4) \AA . The crystal was weak and clearly showed signs of splitting (see Figure S3), but data were collected at 90 K and solved with Superflip.² This structure solved in the space group Pcan with a single **Eu.L** tetramer in the asymmetric unit. In addition to the tetramer, developing the structure showed the presence of NaOTf and additional water molecules. Several triflate anions were visible in the difference map, but refinement was unstable. As a result all the uncoordinated triflate anions were excluded from the final model.

Given the superficial similarity of the unit cells and the relationship between the packing (see Figure S4), additional data were collected to investigate the possibility of phase transitions. The triclinic cell was seen on two other occasions at both 90 K and 250 K and the orthorhombic cell was seen at 100 K at Diamond. This suggests that the different structures are due to differences in the solvent sphere, which is possible as the crystals were taken from a highly saturated solution, the concentration and composition of which would have changed over time, and especially as crystals were removed.

In general, all of the structure solutions were incomplete and needed refinement, Fourier syntheses, and model building techniques to develop the structure. Given the poor quality of the data in general, and the noisiness and lack of high angle data specifically, copious restraints were necessary to maintain sensible geometric parameters and displacement ellipsoids. The tetrameric nature of the structure and high Z' for the worst structures was particularly useful in this regard because it meant there was a high multiplicity for each distance making "same distance" restraints highly effective. In addition, planarity, thermal similarity and vibrational restraints were also used. All three structures were refined to completion using CRYSTALS.⁶ In each case, there were significant solvent accessible voids and the difference Fourier map indicated the presence of diffuse electron density believed to be disordered solvent (and, in the case of the orthorhombic structure, additional sodium triflate). In each case, SQUEEZE⁷ was used to calculate the discrete

⁴ G. Winter, 2010, *J. Appl. Cryst.*, 43, 186-190.

⁵ G. M. Sheldrick, 2015, *Acta Cryst.*, A71, 3-8.

⁶ P. W. Betteridge, J. R. Carruthers, R. I. Cooper, K. Prout and D. J. Watkin, 2003, *J. Appl. Cryst.*, 36, 1487; R. I. Cooper, A. L. Thompson and D. J. Watkin, 2010, *J. Appl. Cryst.*, 43, 1100-1107; P. Parois, R. I. Cooper and A. L. Thompson, 2015, *Chem. Cent. J.*, 9:30.

⁷ A. Spek, 2003, *J. Appl. Cryst.*, 36, 7-13; P. van der Sluis and A. L. Spek, 1990, *Acta Cryst.*, A46, 194-201.

Fourier transform of the void region which were treated as contributions to the A and B parts of the calculated structure factors leaving a void from which the electron density was removed.

Although all three of the final structures are poor there is little doubt of the gross connectivity and despite the issues surrounding each one, the results all support the conclusions drawn in the manuscript. Moreover, the combined weight of all three structures puts the conclusions beyond reasonable doubt. All three structures were finalised (Table S1) and are included in the ESI/CIF which has been deposited with the Cambridge Crystallographic Data Centre (CCDC XXXX-XXXX).

	Eu.L-Monoclinic	Eu.L-Triclinic	Eu.L-Orthorhombic
Data Source	SuperNova	I19-1 at Diamond	XtaLAB Synergy
Crystal system	Monoclinic	Triclinic	Orthorhombic
Formula (excluding void)	C ₁₀₀ H ₁₃₂ Eu ₄ N ₁₆ O ₄₀	C ₁₀₀ H ₁₃₂ Eu ₄ N ₁₆ O ₄₀	C ₁₀₀ H ₁₃₂ Eu ₄ N ₁₆ O ₄₀ .NaOTf.H ₂ O
Cell a /Å	52.668(3)	17.4223(9)	17.9227(7)
Cell b /Å	18.1007(6)	25.1438(15)	32.9420(9)
Cell c /Å	32.7146(17)	33.2547(15)	47.9786(16)
Cell α /°	90	106.177(5)	90
Cell β /°	106.632(6)	90.802(5)	90
Cell γ /°	90	102.807(5)	90
Cell Volume /Å ³	29883(3)	13598.1(13)	28326.9(16)
Space group	P2/c	P1	Pcan
Collection temperature /K	150	100	
Crystal Size /mm	0.10 x 0.22 x 0.40	0.05 x 0.10 x 0.15	0.040 x 0.085 x 0.085
Crystal colour	clear pale colourless	clear pale colourless	clear pale colourless
Z	8	4	8
Z'	2	2	1
λ /Å	1.54184	0.6889	1.54184
Data / restraints / parameters	15564/8786/2881	14186/8786/2881	27811/4401/1525
Void as a %age of Unit cell ⁸	32.0%	24.5	24.2
Δρ(min,max) /e.Å ⁻³	-1.14,2.75	-1.87,4.21	-5.30,8.30
R ₁ [I > 2σ(I)]	0.1773	0.1613	0.1745
wR ₂ [I > 2σ(I)]	0.2135	0.1774	0.4583
Goodness of fit	1.1332	1.1658	0.9996

Table S1. Selected statistics for the data collections and final refinements.

⁸ Calculated using Mercury (C. F. Macrae, I. J. Bruno, J. A. Chisholm, P. R. Edgington, P. McCabe, E. Pidcock, L. Rodriguez-Monge, R. Taylor, J. van de Streek & P. A. Wood, 2008, *J. Appl. Cryst.*, 41, 466-470).

NMR spectra of synthesised compounds

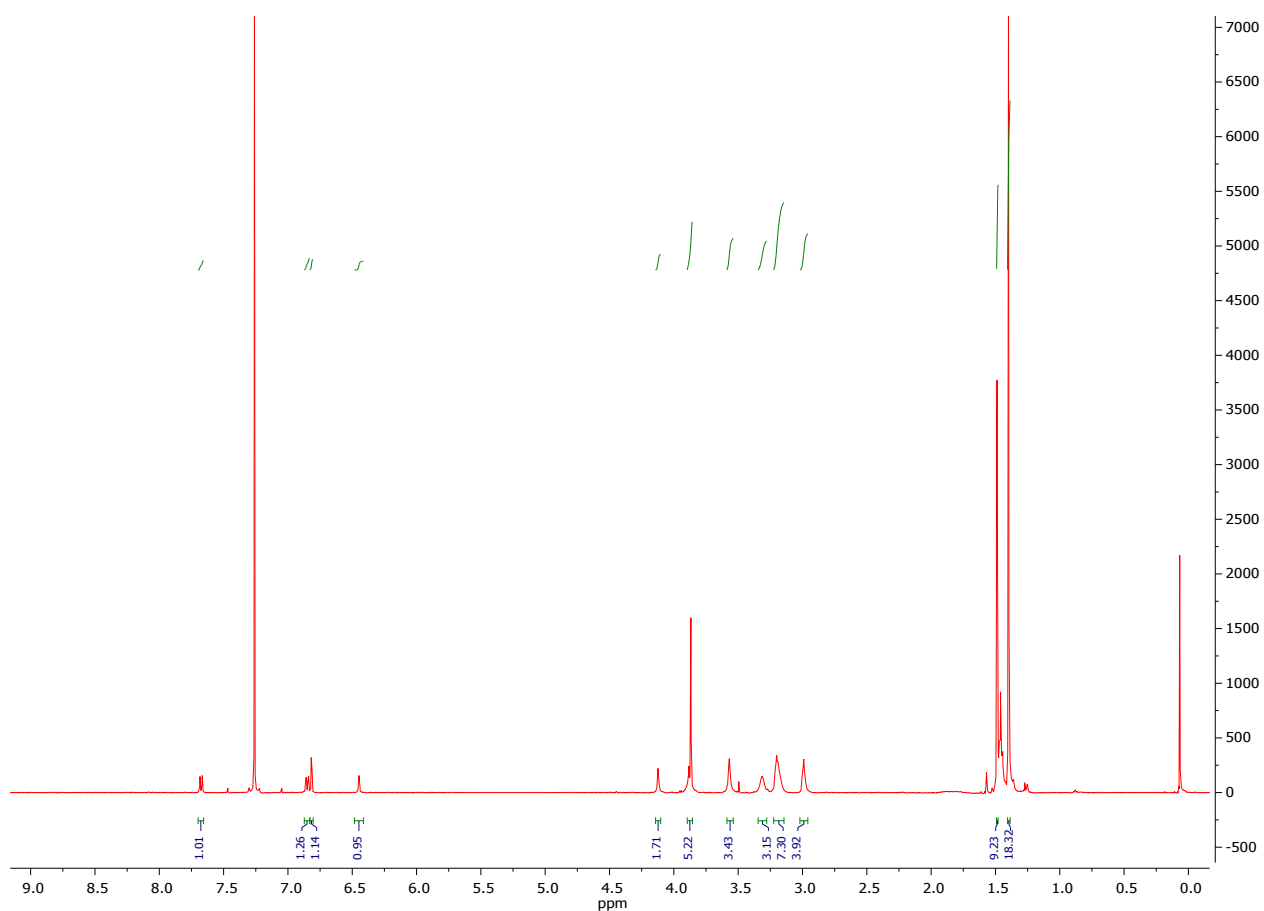


Figure S1. ¹H-NMR spectrum of preligand 3 (500 MHz). Signal at 1.21 and 3.48 ppm are residual diethylether.

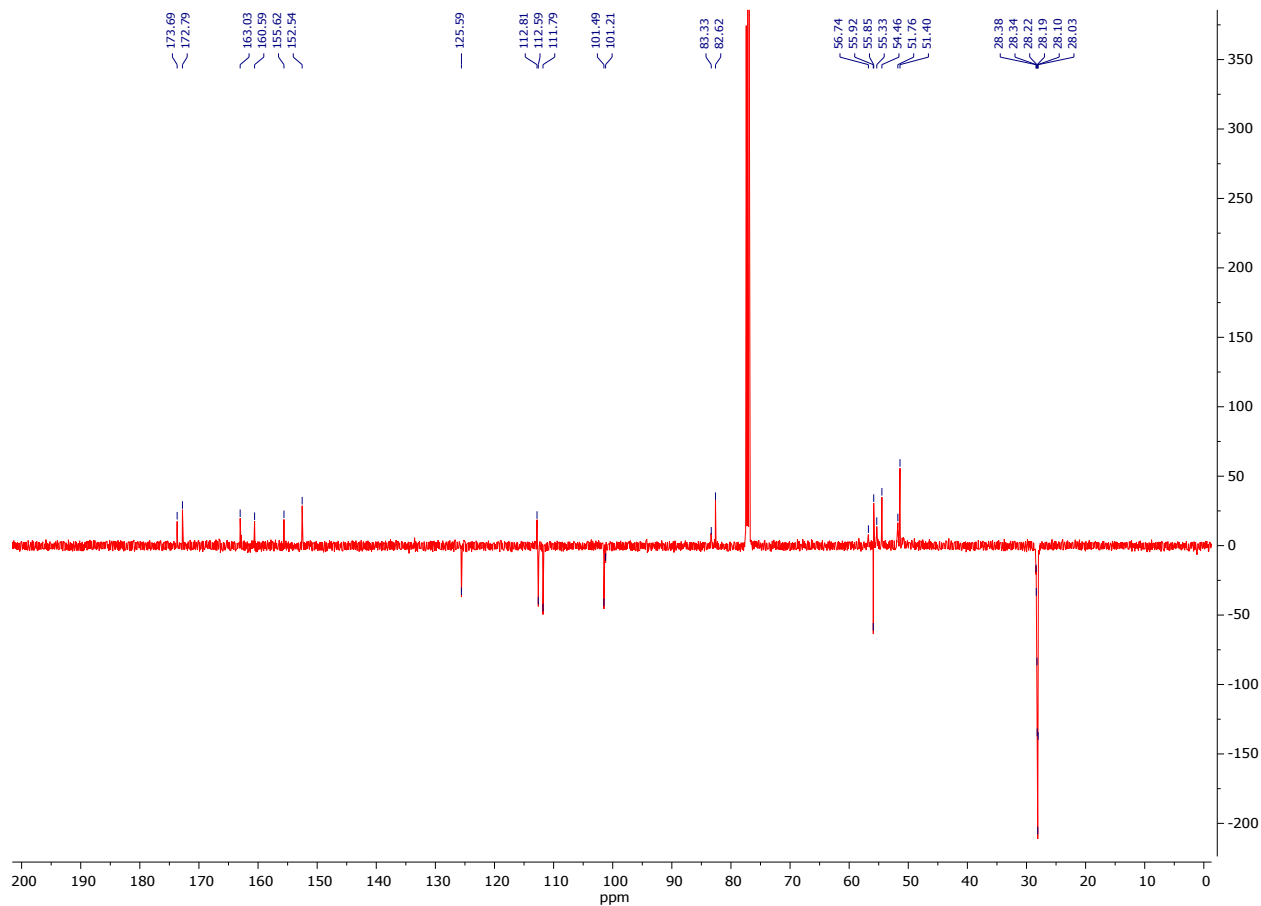


Figure S2. ^{13}C -NMR spectrum of preligand **3** (126 MHz CDCl_3).

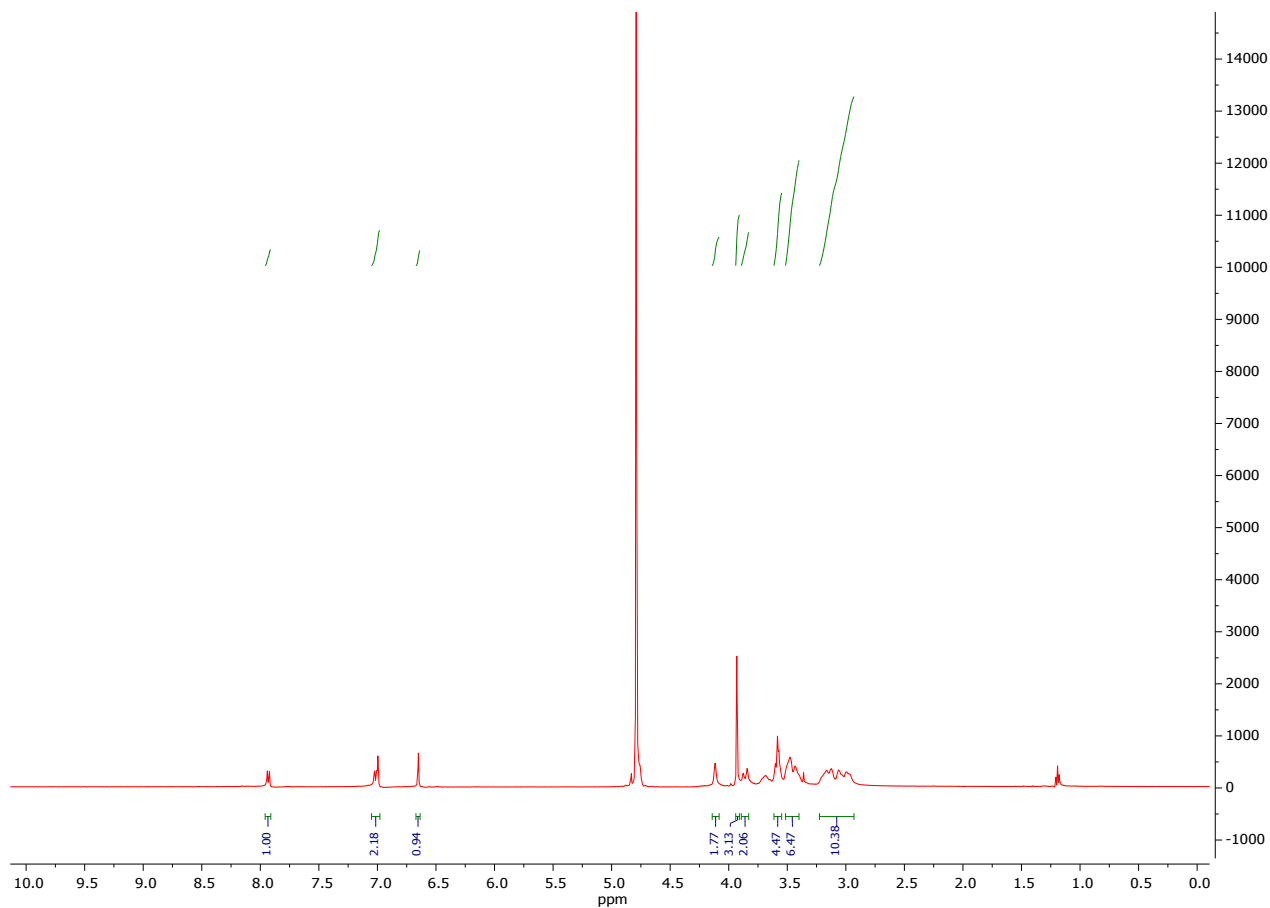


Figure S3. ¹H-NMR spectrum of the ligand L (500 MHz D₂O). Signal at 1.12 ppm residual diethylether.

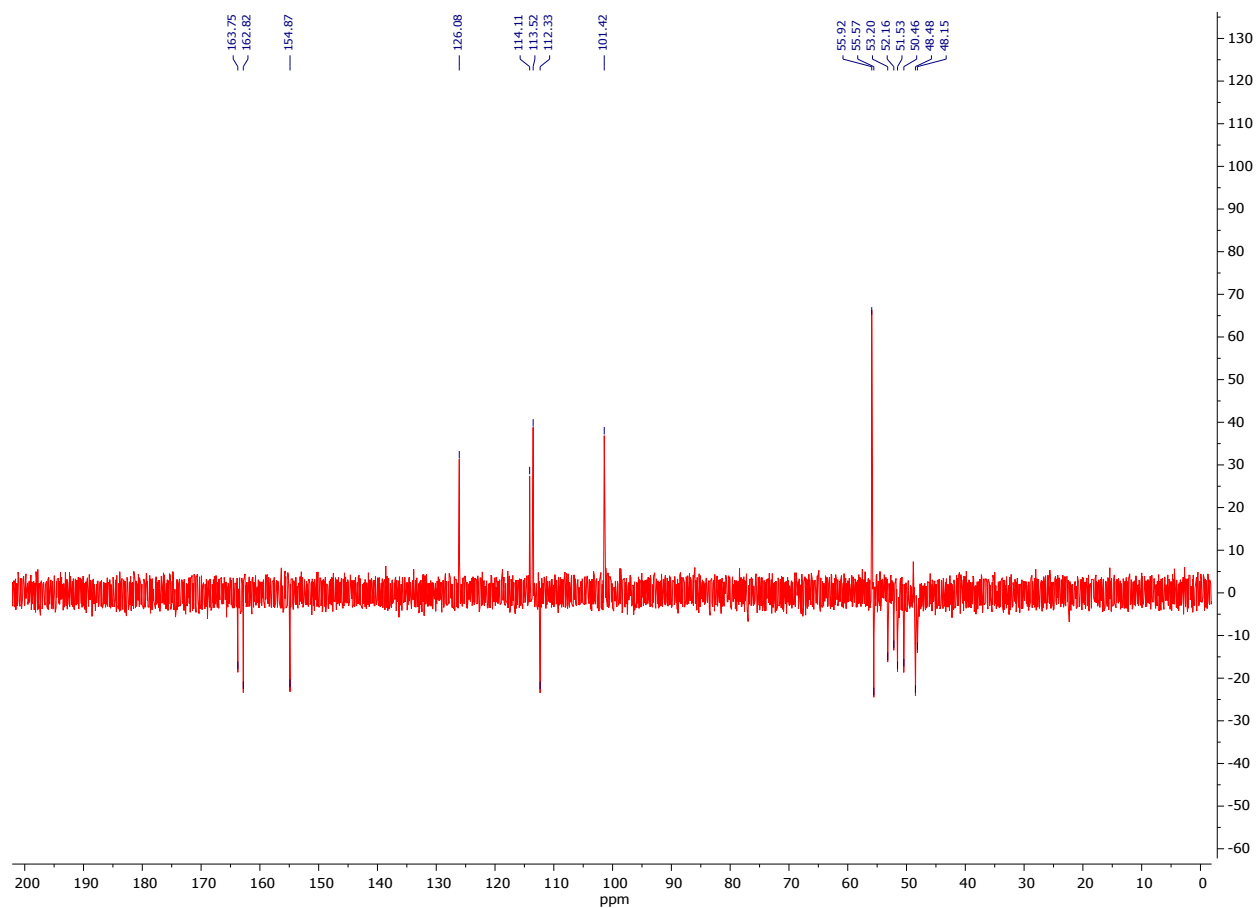


Figure S4. ^{13}C NMR spectrum of the ligand L (126 MHz D_2O). 4 quaternary carbon signals from the coumarin are missing.

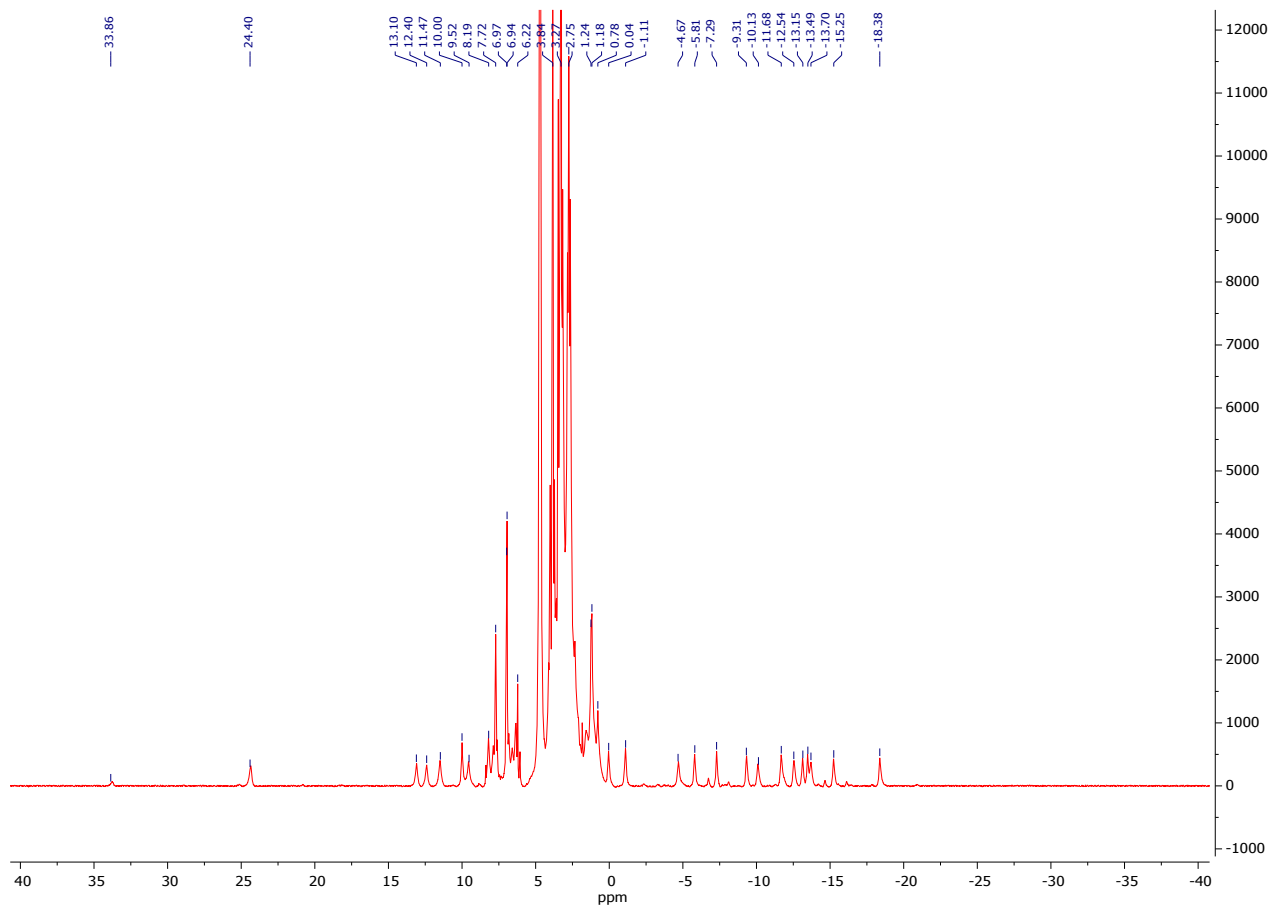


Figure S5. $^1\text{H-NMR}$ spectrum of **Eu.L** (500 MHz D_2O).

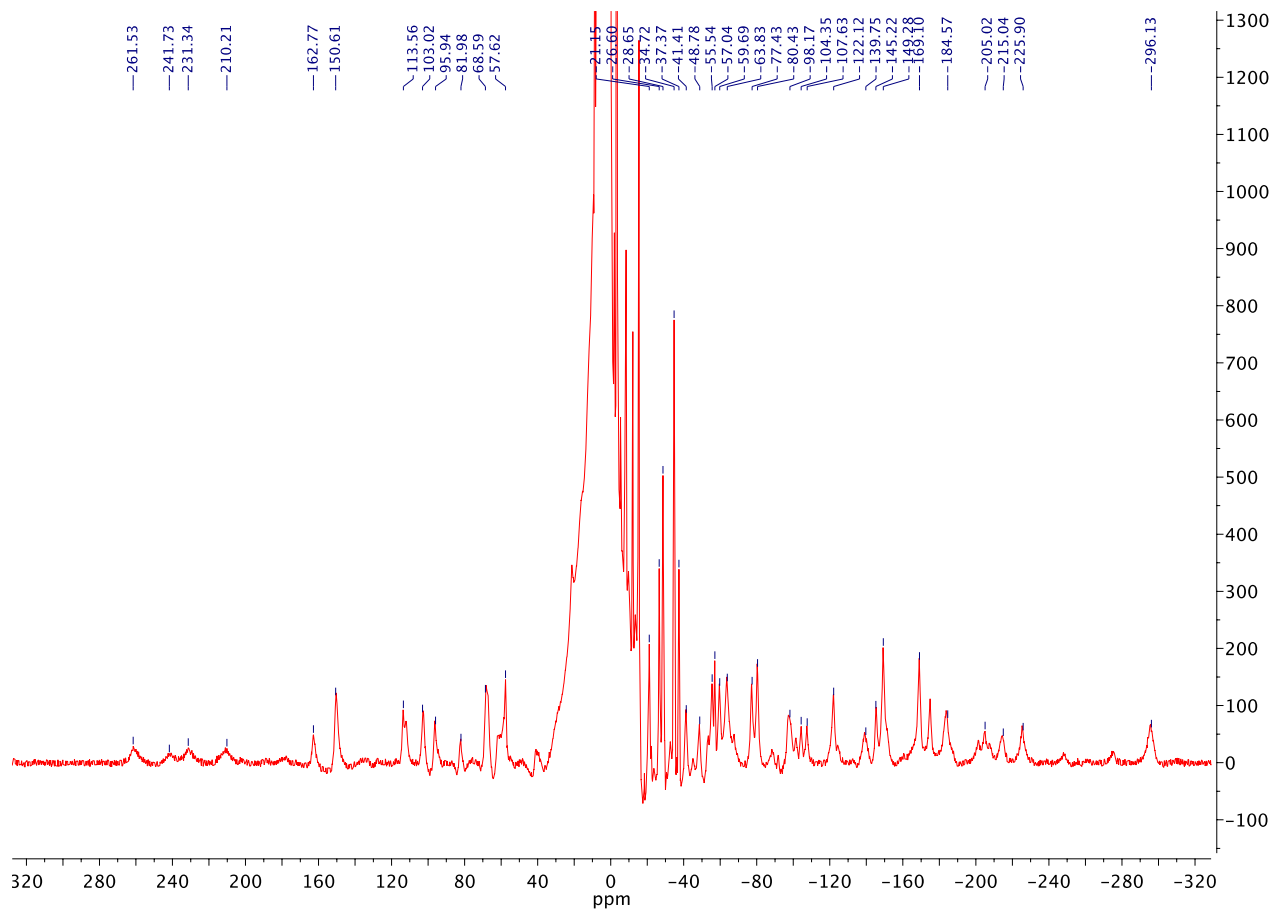


Figure S6. ^1H NMR spectrum of **Tb.L** (500 MHz D_2O)

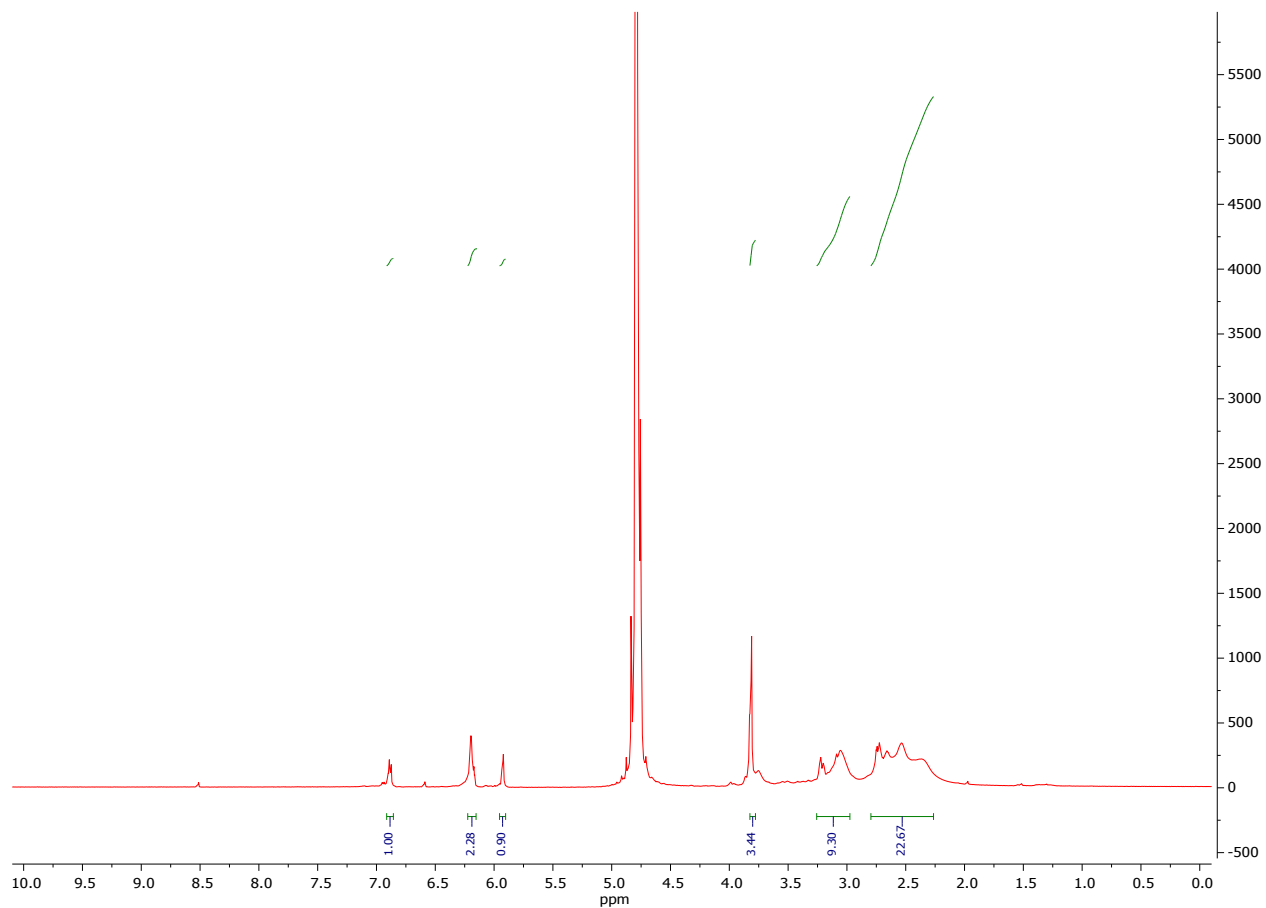


Figure S7. ¹H-NMR spectrum of Y.L (500 MHz D₂O).

Optical Spectroscopy:

Absorption Spectra

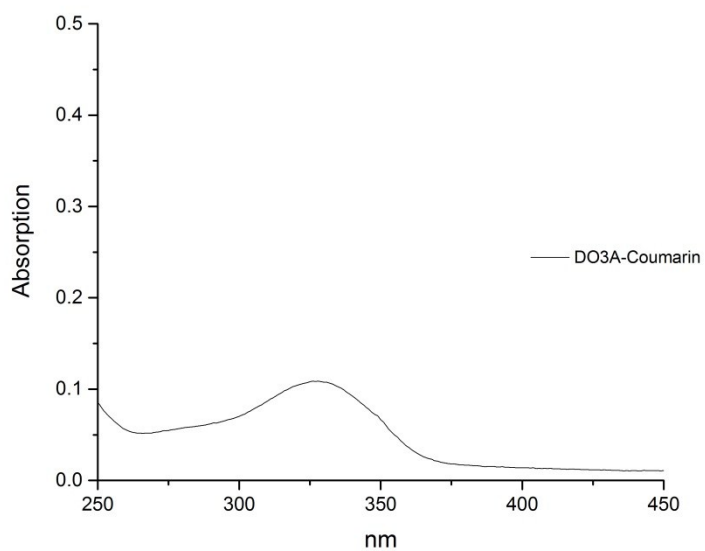


Figure S8. Absorption spectrum of a 12.7 μM solution of DO3A-Coumarin (L) in HEPES Buffer pH 7.4

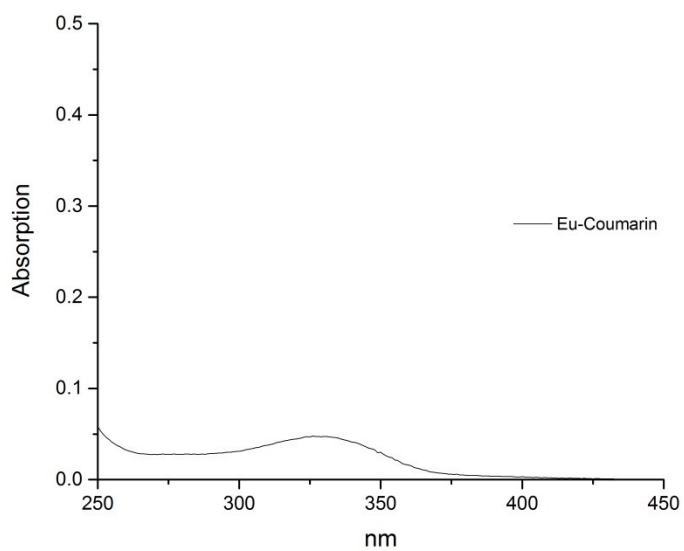


Figure S9. Absorption spectrum of a 12.7 μM solution of **Eu.L** in HEPES Buffer pH 7.4

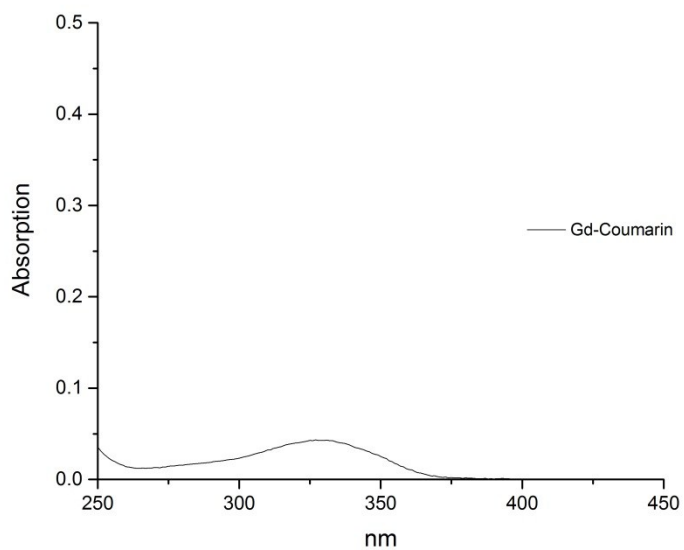


Figure S10. Absorption spectrum of a 12.7 μM solution of **Gd.L** in HEPES Buffer pH 7.4

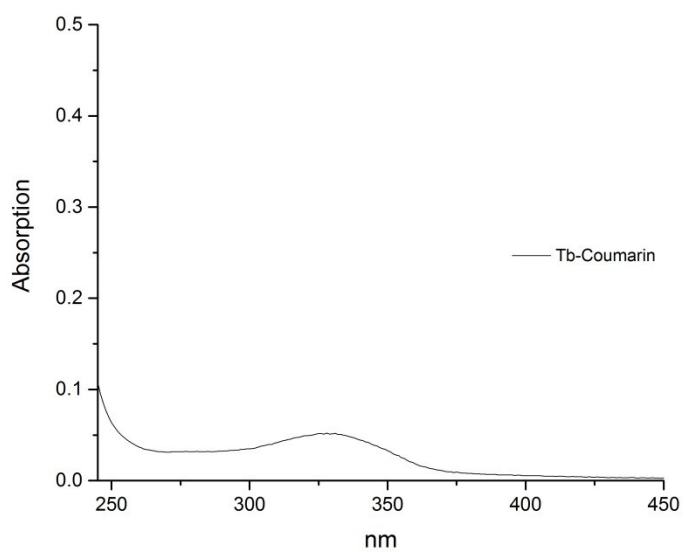


Figure S11. Absorption spectrum of a 12.7 μM solution of **Tb.L** in HEPES Buffer pH 7.4

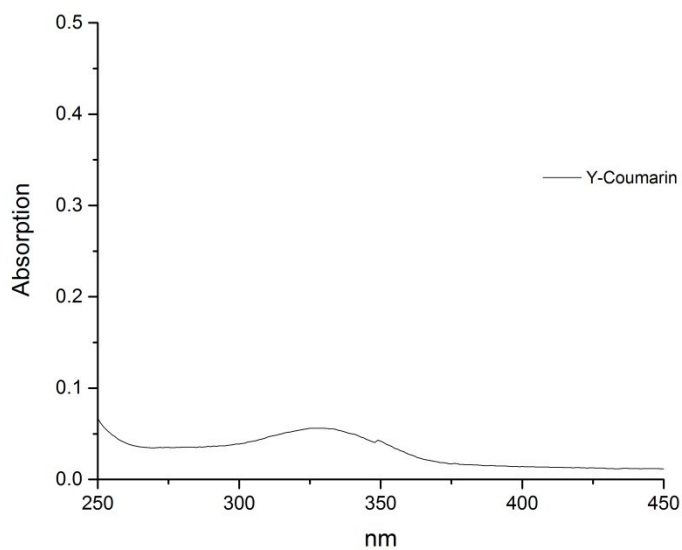


Figure S12. Absorption spectrum of a 12.7 μM solution of Y.L in HEPES Buffer pH 7.4

Excitation Spectra

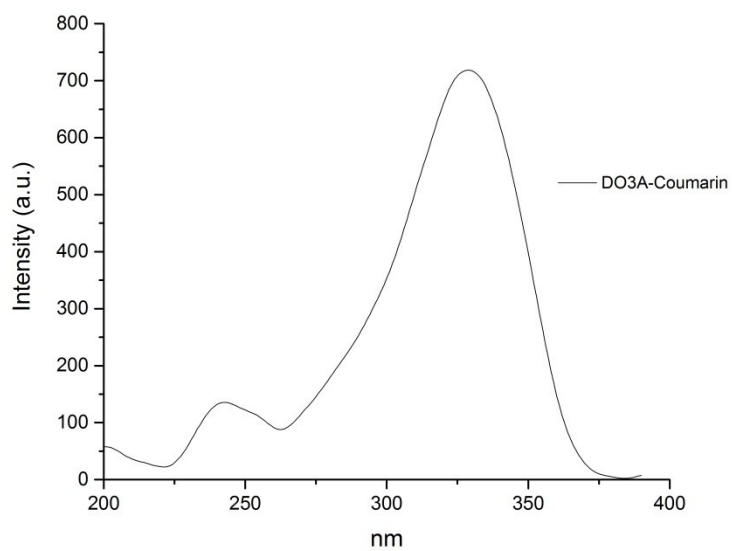


Figure S13. Excitation spectrum of a 12.7 μM solution of DO3A-Coumarin (L) in HEPES Buffer pH 7.4. Emission followed at 325 nm slits 5/2.5

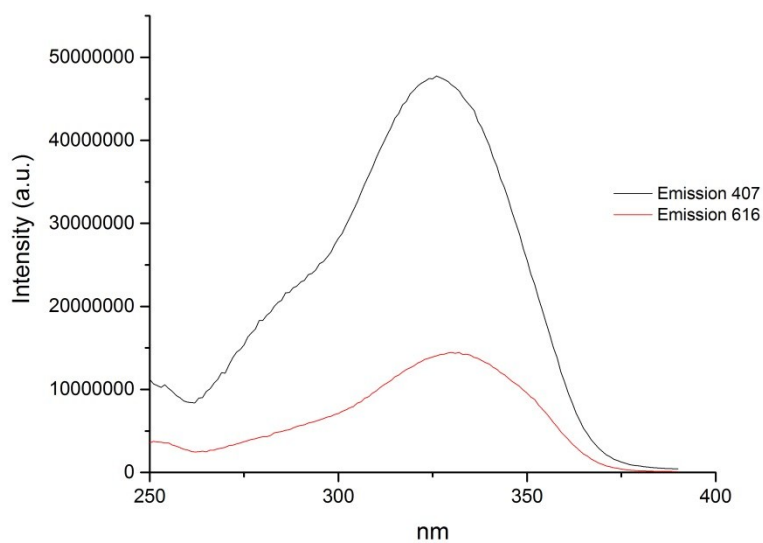


Figure S14. Excitation spectrum of a 12.7 μM solution of **Eu.L** in HEPES Buffer pH 7.4. Emission followed at 407 and 616 nm slits 5/2.5.

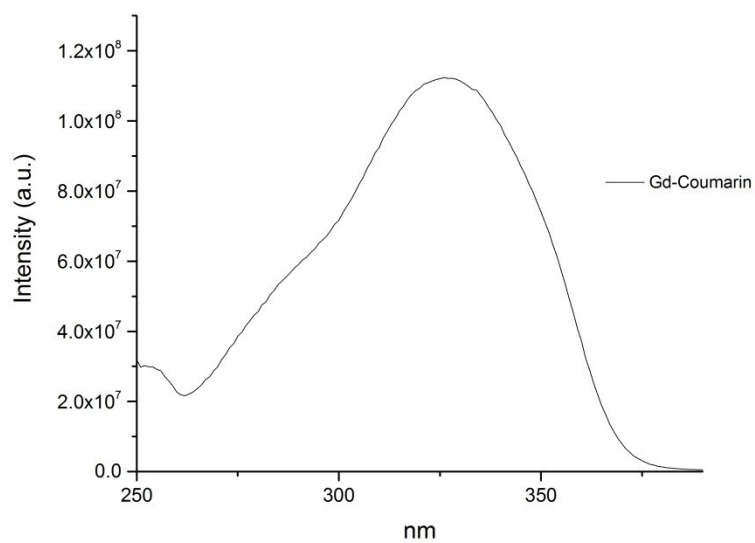


Figure S15. Excitation spectrum of a 12.7 μM solution of **Gd.L** in HEPES Buffer pH 7.4, emission followed at 407 nm slits 5/2.5.

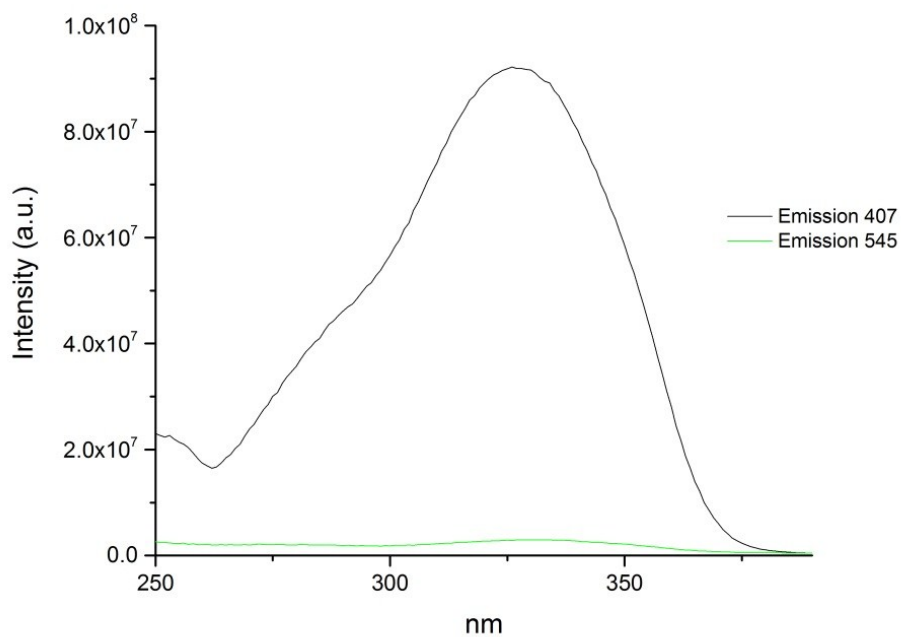


Figure S16. Excitation spectrum of a 12.7 μM solution of **Tb.L** in HEPES Buffer pH 7.4, emission followed at 407 and 545 nm slits 5/2.5.

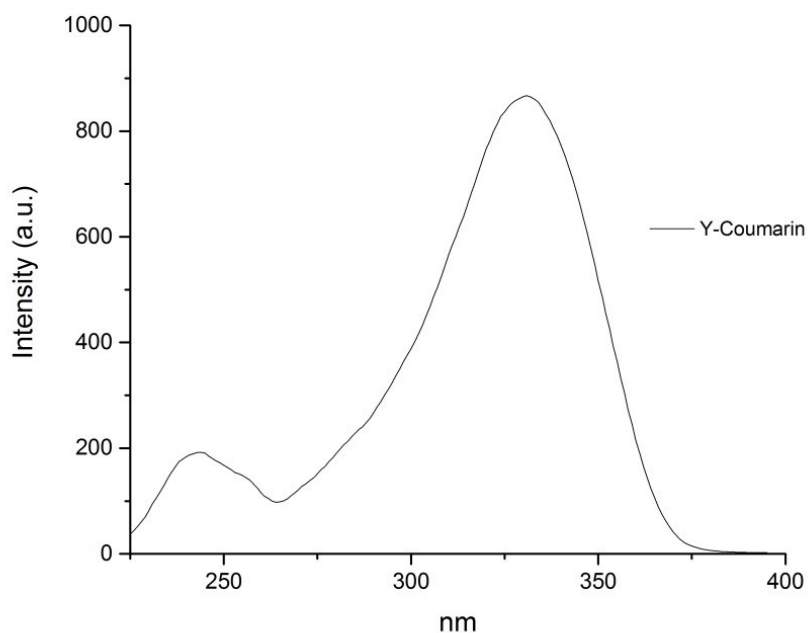


Figure S17. Excitation spectrum of a 12.7 μM solution of **Y.L** in HEPES Buffer pH 7.4, emission followed at 407 nm slits 5/2.5.

Emission Spectra

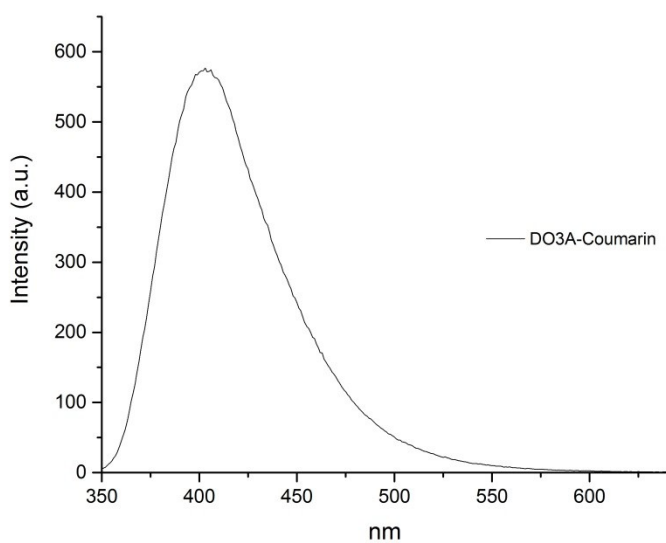


Figure S18. Emission spectrum of a 12.7 μM solution of DO3A-Coumarin (**L**) in HEPES Buffer pH 7.4 Excitation 325 nm slits 2.5/5.

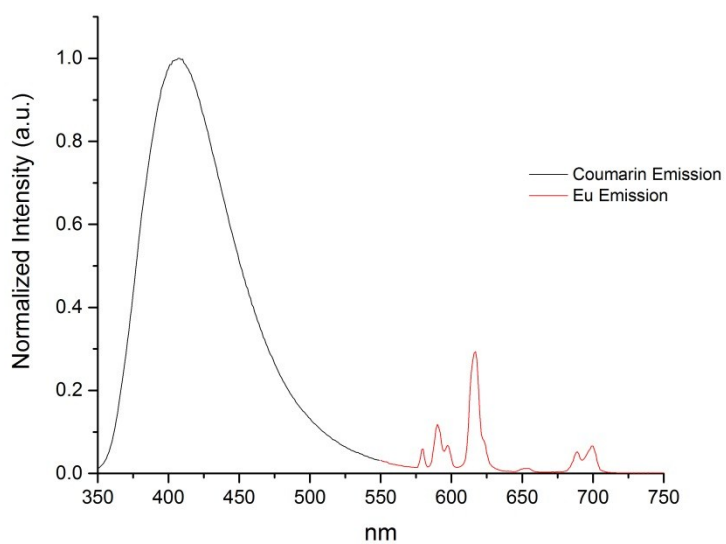


Figure S19. Emission spectrum of a 12.7 μM solution of **Eu.L** in HEPES Buffer pH 7.4, excitation at 325 nm slits 2.5/5.

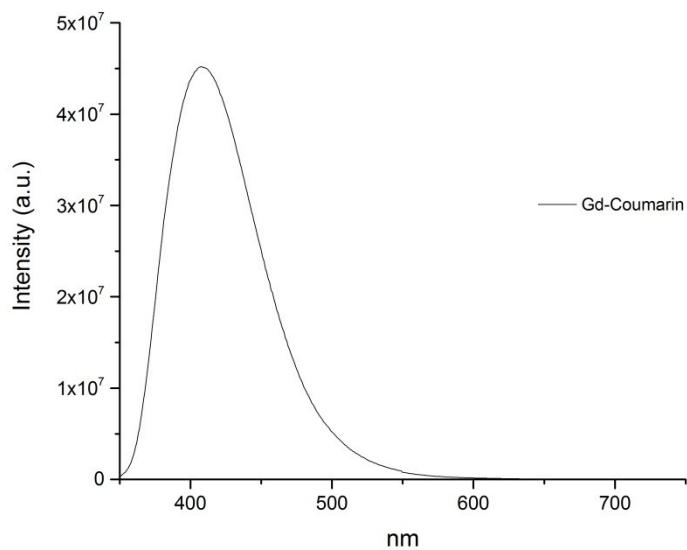


Figure S20. Emission spectrum of a 12.7 μM solution of **Gd.L** in HEPES Buffer pH 7.4, excitation at 325 nm slits 2.5/5.

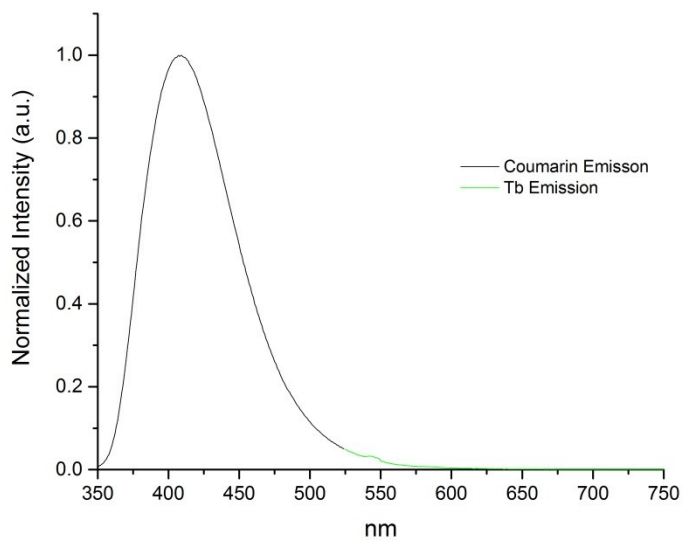


Figure S21. Emission spectrum of a 12.7 μM solution of **Tb.L** in HEPES Buffer pH 7.4, excitation at 325 nm slits 2.5/5.

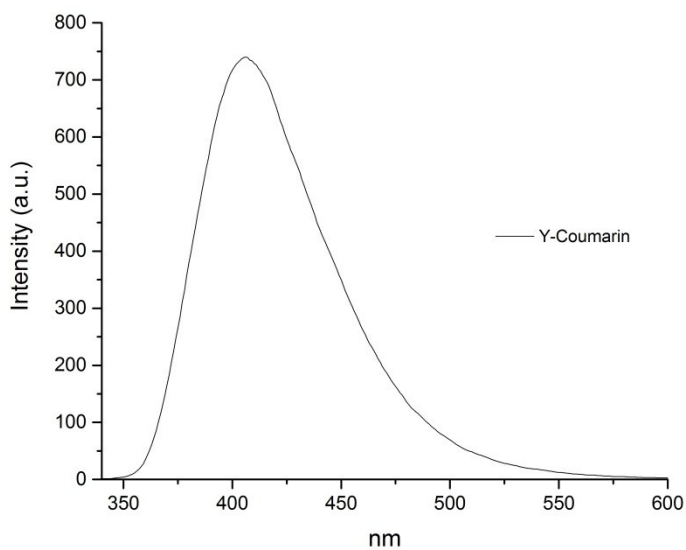


Figure S22. Emission spectrum of a 12.7 μM solution of **Y.L** in HEPES Buffer pH 7.4, excitation at 325 nm slits 2.5/5.

Phosphorescence spectra

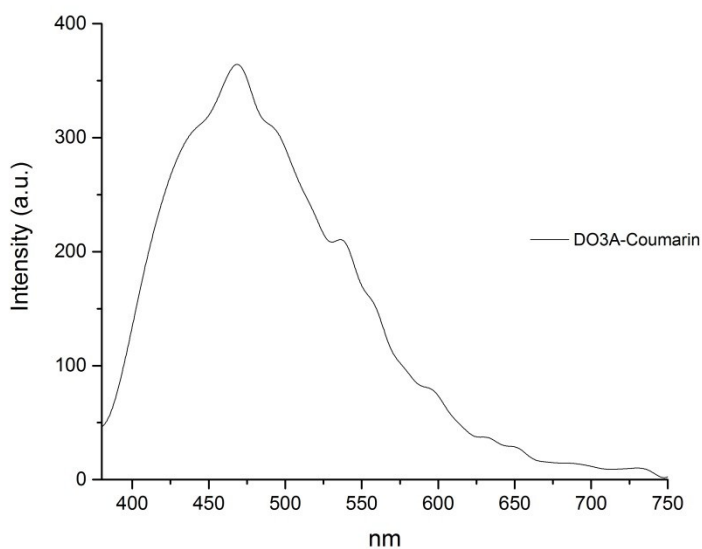


Figure S23. Phosphorescence emission spectrum of a 12.7 μM solution of DO3A-Coumarin (**L**) in HEPES Buffer pH 7.4 at 77 K, excitation at 325 nm slits 10/20. Total decay time 0.02 s, Delay 0.5 ms and gate time 10 ms.

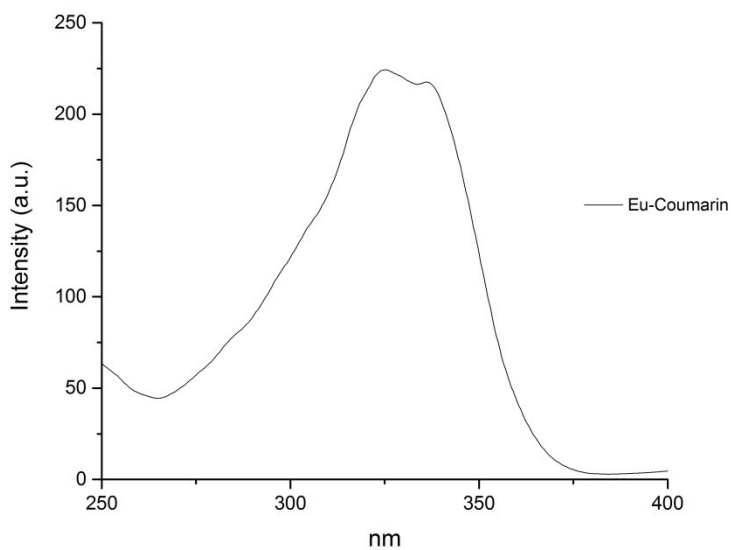


Figure S24. Phosphorescence excitation spectrum of a 12.7 μM solution of **Eu.L** in HEPES Buffer pH 7.4 at 77 K, emission followed at 700 nm slits 20/5. Total decay time 0.02 s, Delay 0.5 ms and gate time 3 ms.

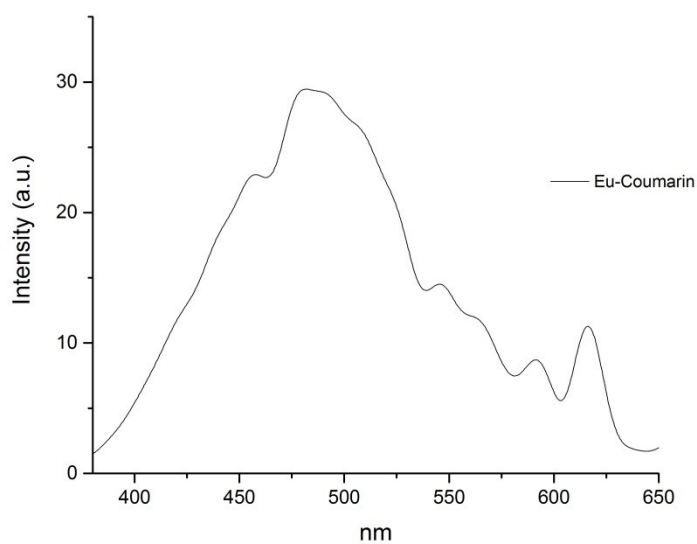


Figure S25. Phosphorescence emission spectrum of a 12.7 μM solution of **Eu.L** in HEPES Buffer pH 7.4 at 77 K, excitation at 325 nm slits 20/5. Total decay time 0.02 s, Delay 0.5 ms and gate time 3 ms.

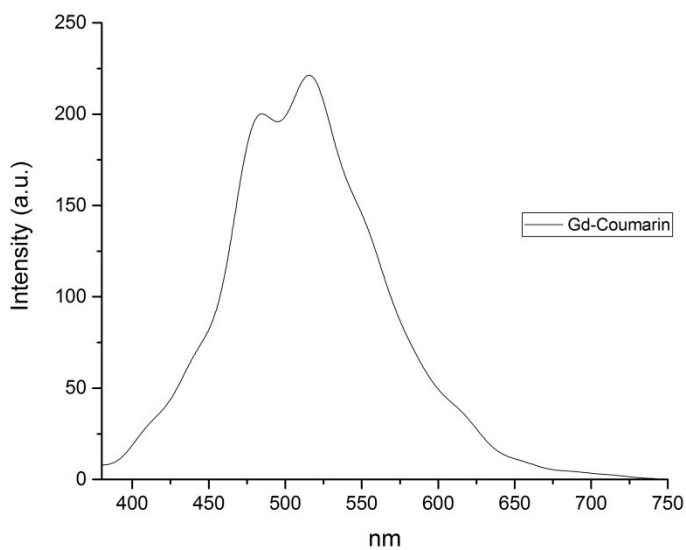


Figure S26. Phosphorescence emission spectrum of a 12.7 μM solution of **Gd.L** in HEPES Buffer pH 7.4 at 77 K, excitation at 325 nm slits 20/10. Total decay time 0.04 s, Delay 7 ms and gate time 30 ms.

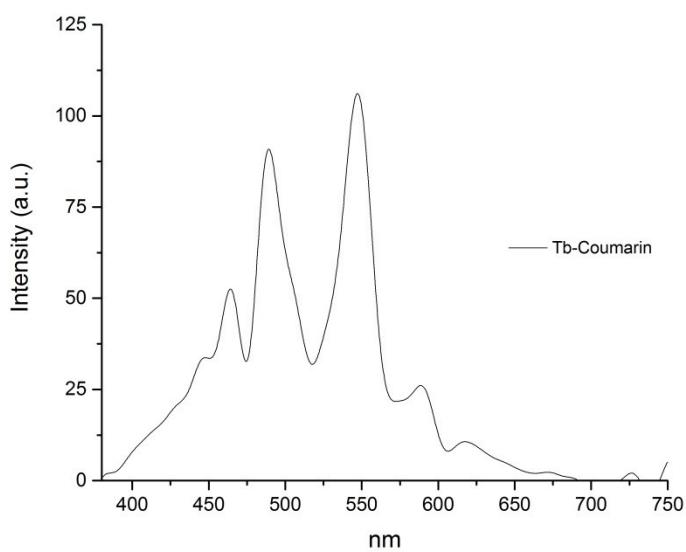


Figure S27. Phosphorescence emission spectrum of a 12.7 μM solution of **Tb.L** in HEPES Buffer pH 7.4 at 77 K, excitation at 325 nm slits 5/10. Total decay time 0.02 s, Delay 1 ms and gate time 15 ms.

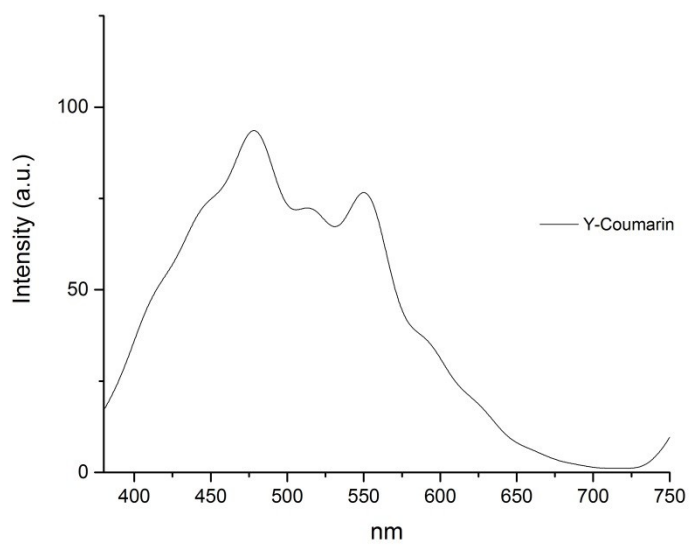


Figure S28. Phosphorescence emission spectrum of a 12.7 μM solution of **Y.L** in HEPES Buffer pH 7.4 at 77 K, excitation at 325 nm slits 10/20. Total decay time 0.02 s, Delay 0.5 ms and gate time 10 ms.

Quantum Yield determination

Quantum yields were determined by the optically dilute method using eq. S1, where Φ is the fluorescence quantum yield, $Grand$ the gradient from the plot of integrated fluorescence intensity vs absorbance, and η the refractive index of the solvent. The subscripts ST and X denote standard and the sample respectively.

$$\Phi_X = \Phi_{ST} \left(\frac{Grand_X}{Grand_{ST}} \right) \left(\frac{\eta_X^2}{\eta_{ST}^2} \right) \quad (S1)$$

For quantum yield calculations, an excitation wavelength of 325 nm was utilized for both the reference and sample. Plotting the integrated fluorescence intensity versus absorbance at 325 nm yields a linear plot with a slope/gradient proportional to the quantum yield of the sample Φ_X . Absolute values are calculated using a standard sample which have a fixed and know fluorescence quantum yield value. Quinine sulfate in 0.5 M sulfuric acid was used as the reference ($\Phi_{ST} = 0.546$). As both sample and reference are measured in the same solvent the refractive index term of the equation equals one can be omitted.

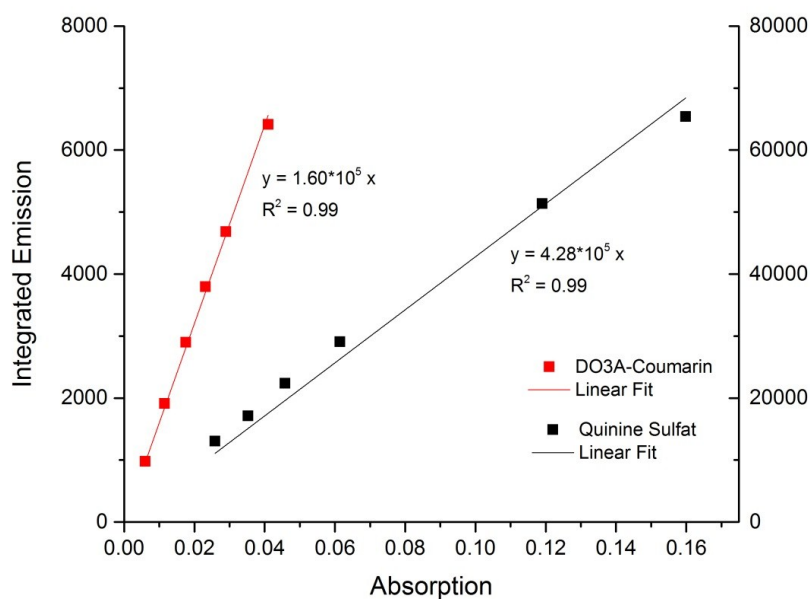


Figure S29. Quantum yield determination for DO3A-Coumarin (L) at pH 7.4 (0.1 M HEPES Buffer). The red line is a linear fit to the data for the sample and the black line is a linear fit for the data for the reference quinine sulfate.

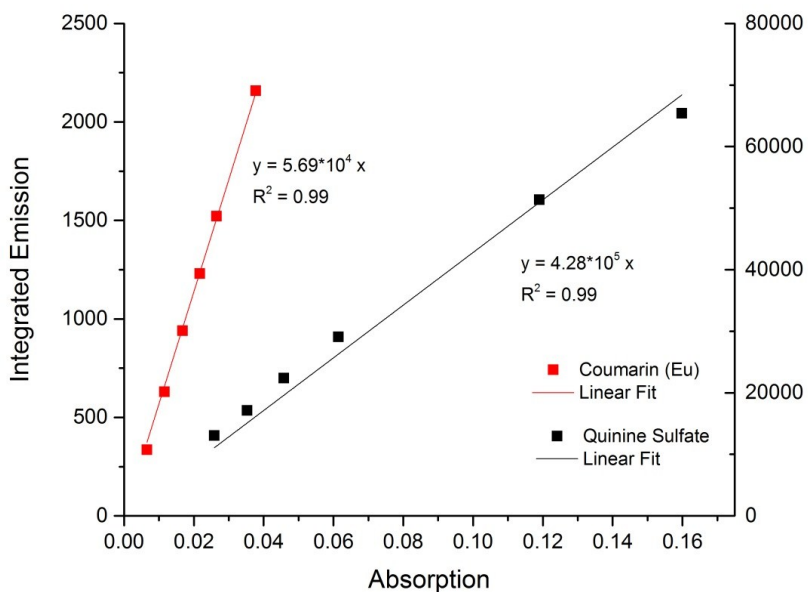


Figure S30. Quantum yield determination for Coumarin (Eu) emission at pH 7.4 (0.1 M HEPES Buffer). The red line is a linear fit to the data for the sample and the black line is a linear fit for the data for the reference quinine sulfate.

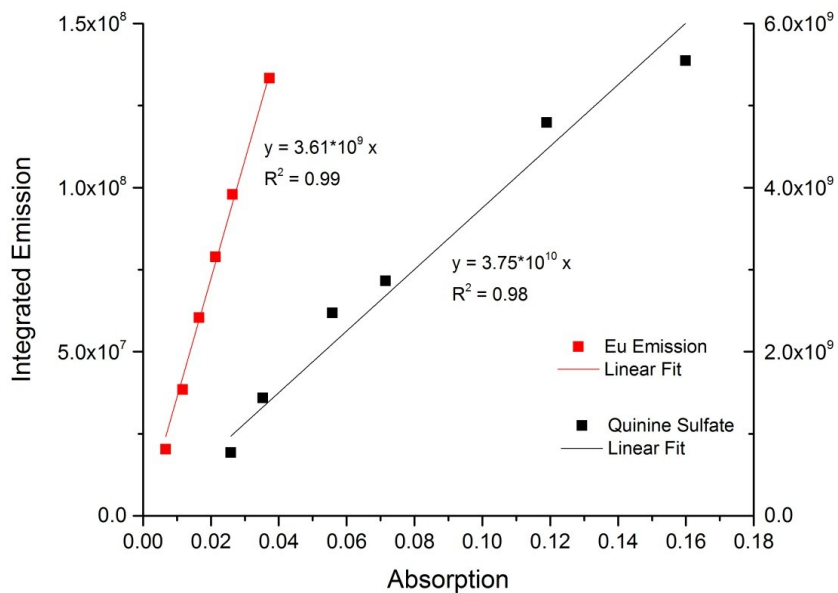


Figure S31. Quantum yield determination for Eu centered emission at pH 7.4 (0.1 M HEPES Buffer). The red line is a linear fit to the data for the sample and the black line is a linear fit for the data for the reference quinine sulfate.

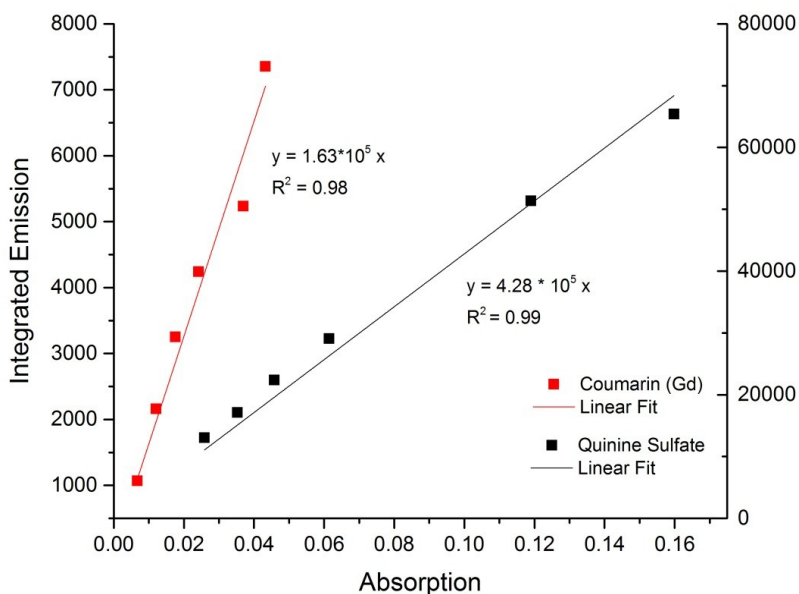


Figure S32. Quantum yield determination for Coumarin (Gd) emission at pH 7.4 (0.1 M HEPES Buffer). The red line is a linear fit to the data for the sample and the black line is a linear fit for the data for the reference quinine sulfate.

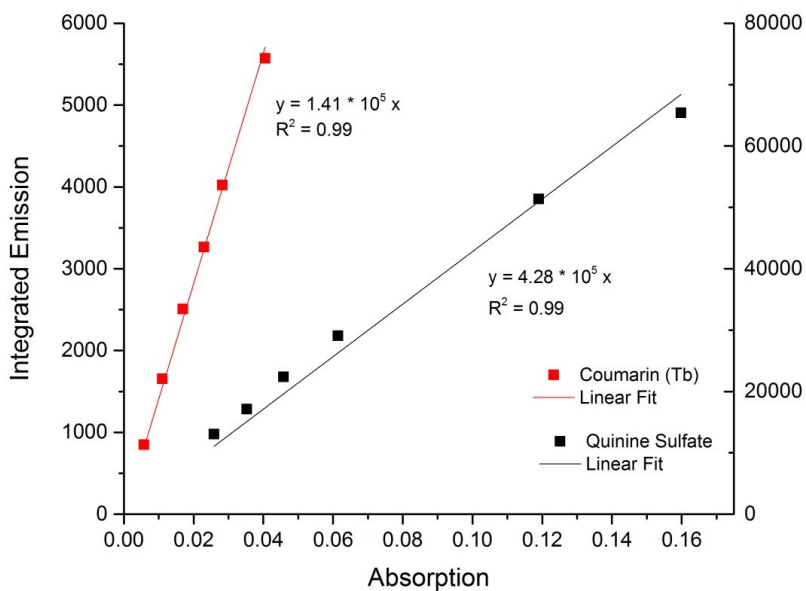


Figure S33. Quantum yield determination for Coumarin (Tb) emission at pH 7.4 (0.1 M HEPES Buffer). The red line is a linear fit to the data for the sample and the black line is a linear fit for the data for the reference quinine sulfate.

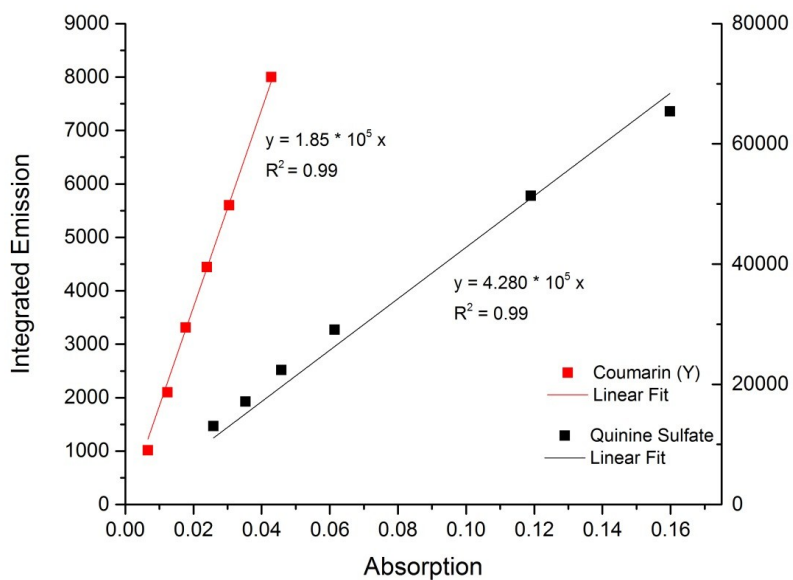
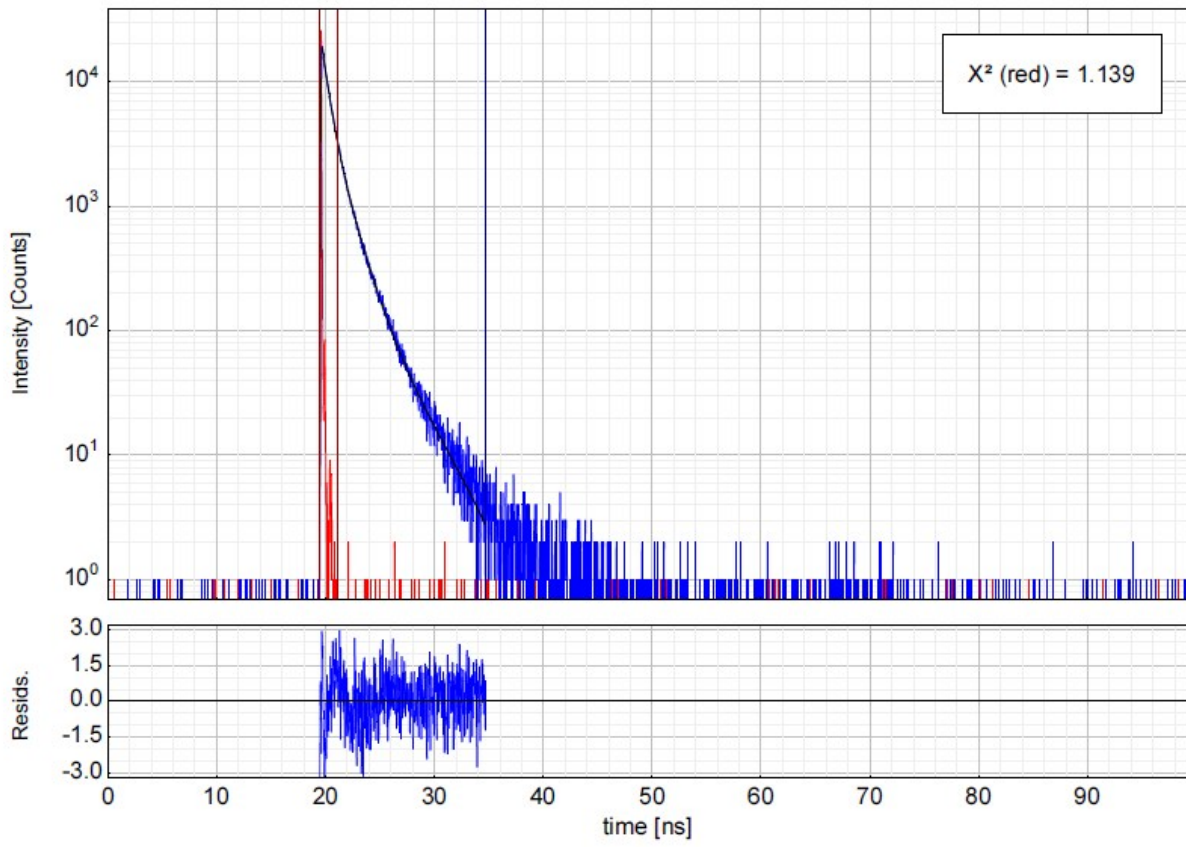


Figure 34. Quantum yield determination for Coumarin (Y) emission at pH 7.4 (0.1 M HEPES Buffer). The red line is a linear fit to the data for the sample and the black line is a linear fit for the data for the reference quinine sulfate.

Fluorescence & Luminescence Lifetime decays and fits

DO3A-Coumarin – H₃.L



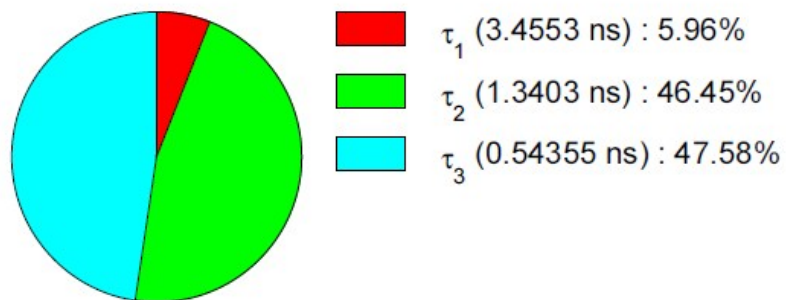
Parameter	Value	Conf. Lower	Conf. Upper	Conf. Estimation
A ₁ [Cnts]	318.7	-93.3	+93.3	Fitting
τ ₁ [ns]	3.4553	-0.0481	+0.0597	Support Plane
A ₂ [Cnts]	6400	-424	+424	Fitting
τ ₂ [ns]	1.3403	-0.0115	+0.0250	Support Plane
A ₃ [Cnts]	16163	-1000	+1000	Fitting
τ ₃ [ns]	0.54355	-0.00377	+0.00662	Support Plane
Bkgr. Dec [Cnts]	-1.40	-5.28	+5.28	Fitting
Bkgr. IRF [Cnts]	-9.8	-25.8	+25.8	Fitting
Shift IRF [ns]	0.62766	-0.00685	+0.00685	Fitting
A _{Scat} [Cnts]	-14740	-4480	+4480	Fitting

Average Lifetime:

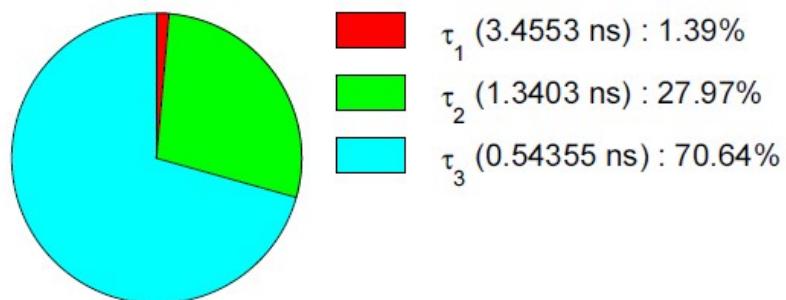
$$\tau_{Av,1} = 1.0873 \text{ ns (intensity weighted)}$$

$$\tau_{Av,2} = 0.8070 \text{ ns (amplitude weighted)}$$

Fractional Intensities of the Positive Decay Components:



Fractional Amplitudes of the Positive Decay Components:



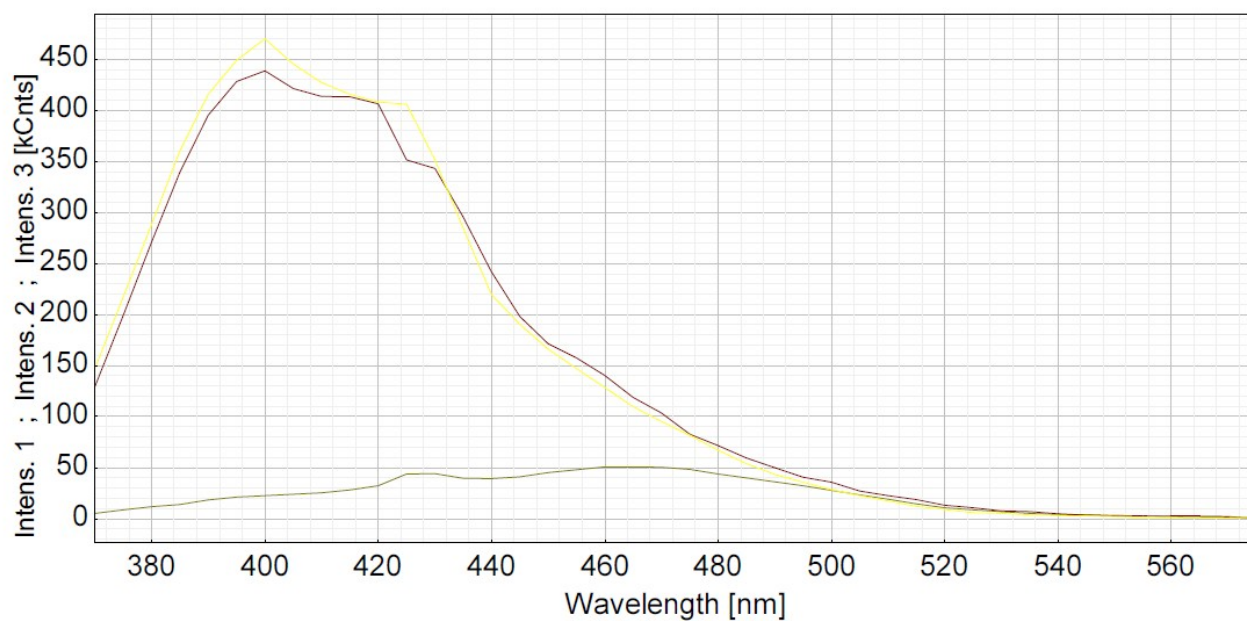
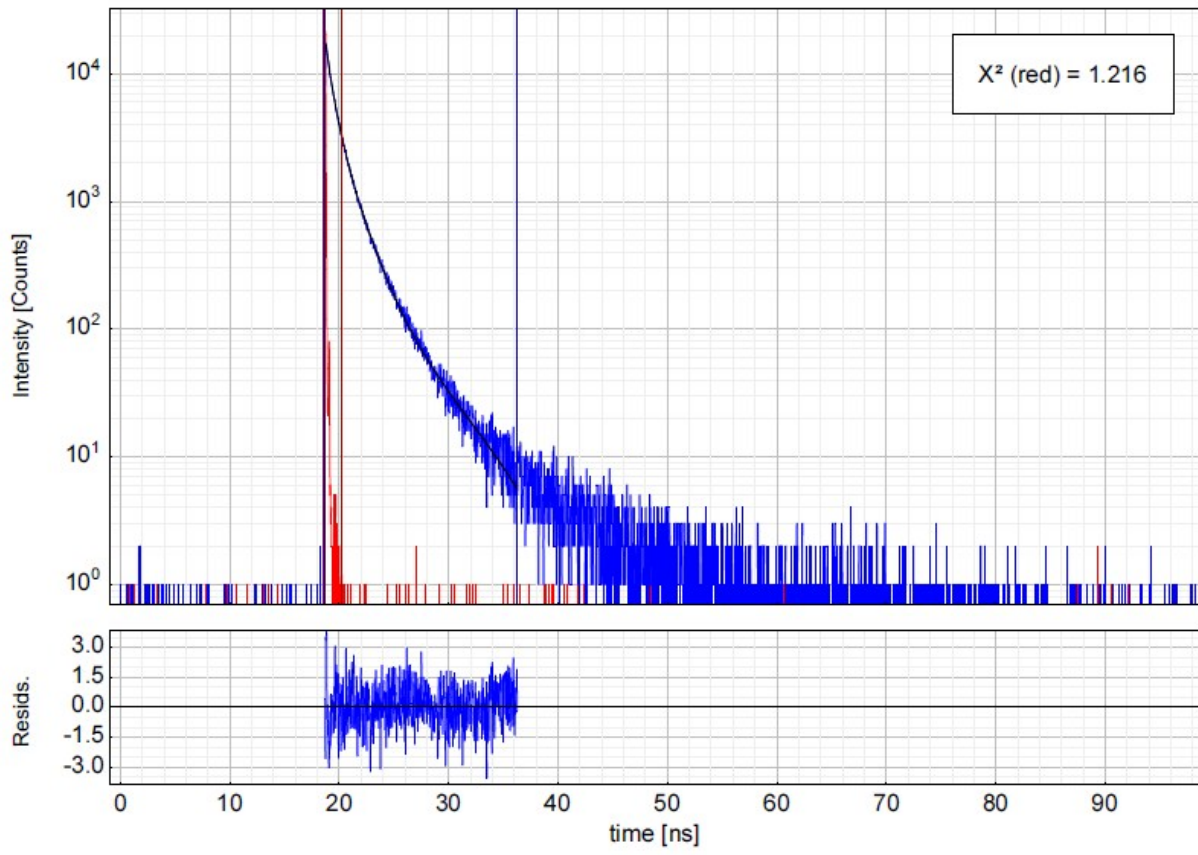


Figure S35. Fluorescence decay profile observed for DO3A-Coumarin ($H_3.L$) in HEPES Buffer pH 7.4. Top, time-resolved emission decay profile. Middle, result of global fit from time resolved emission spectra. Bottom, emission spectra deconvoluted using three lifetime components. The data was fitted to a triexponential decay to determine the associated lifetimes.



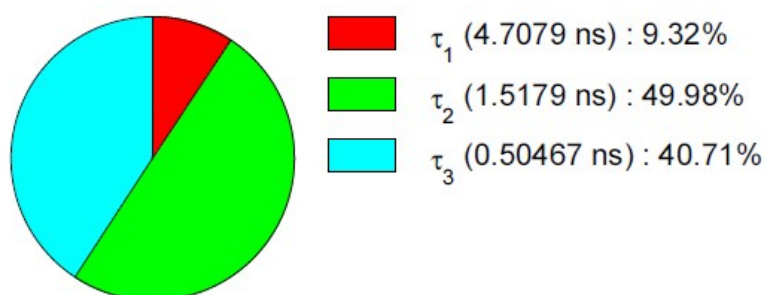
Parameter	Value	Conf. Lower	Conf. Upper	Conf. Estimation
A ₁ [Cnts]	329.6	-79.0	+79.0	Fitting
τ ₁ [ns]	4.7079	-0.0508	+0.0519	Support Plane
A ₂ [Cnts]	5485	-424	+424	Fitting
τ ₂ [ns]	1.5179	-0.0126	+0.0130	Support Plane
A ₃ [Cnts]	13430	-1200	+1200	Fitting
τ ₃ [ns]	0.50467	-0.00506	+0.00523	Support Plane
Bkgr. Dec [Cnts]	-2.92	-7.52	+7.52	Fitting
Bkgr. IRF [Cnts]	-53.2	-35.2	+35.2	Fitting
Shift IRF [ns]	-0.9766	-0.0162	+0.0162	Fitting
A _{Scat} [Cnts]	4810	-8820	+8820	Fitting

Average Lifetime:

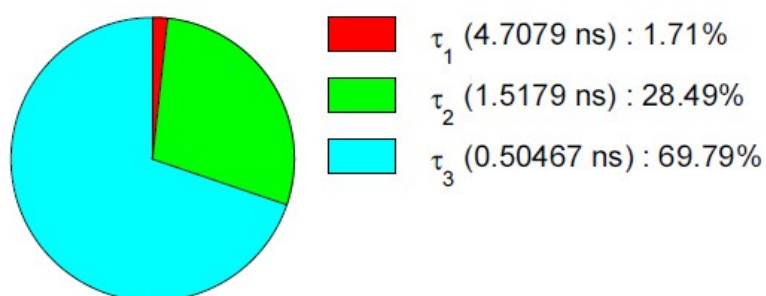
$$\tau_{Av,1} = 1.4026 \text{ ns (intensity weighted)}$$

$$\tau_{Av,2} = 0.8653 \text{ ns (amplitude weighted)}$$

Fractional Intensities of the Positive Decay Components:



Fractional Amplitudes of the Positive Decay Components:



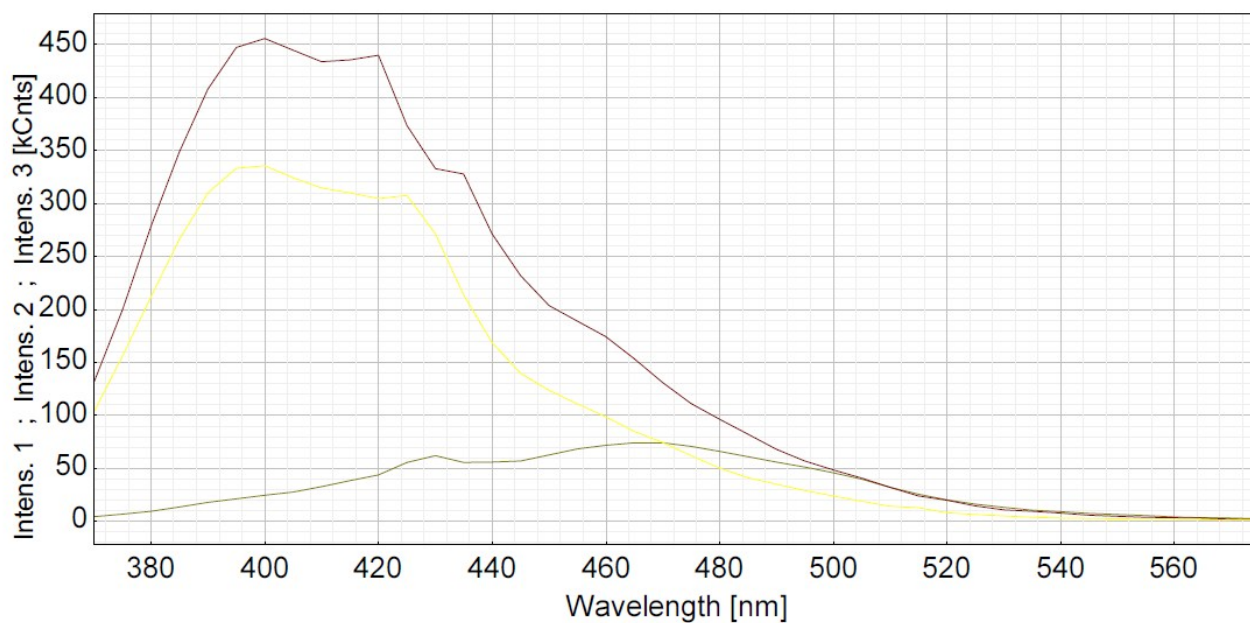


Figure S36. Fluorescence decay profile observed for DO3A-Coumarin (L) in D₂O HEPES Buffer pH 7.4. Top, time-resolved emission decay profile. Middle, result of global fit from time resolved emission spectra. Bottom, emission spectra deconvoluted using three lifetime components. The data was fitted to a triexponential decay to determine the associated lifetimes.

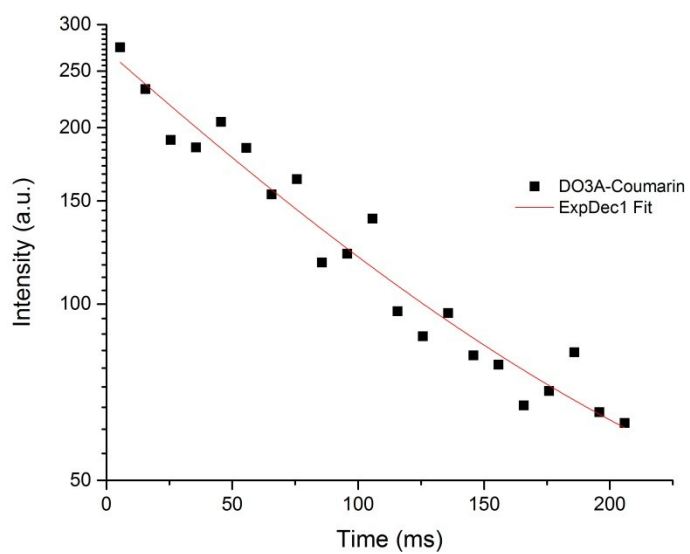
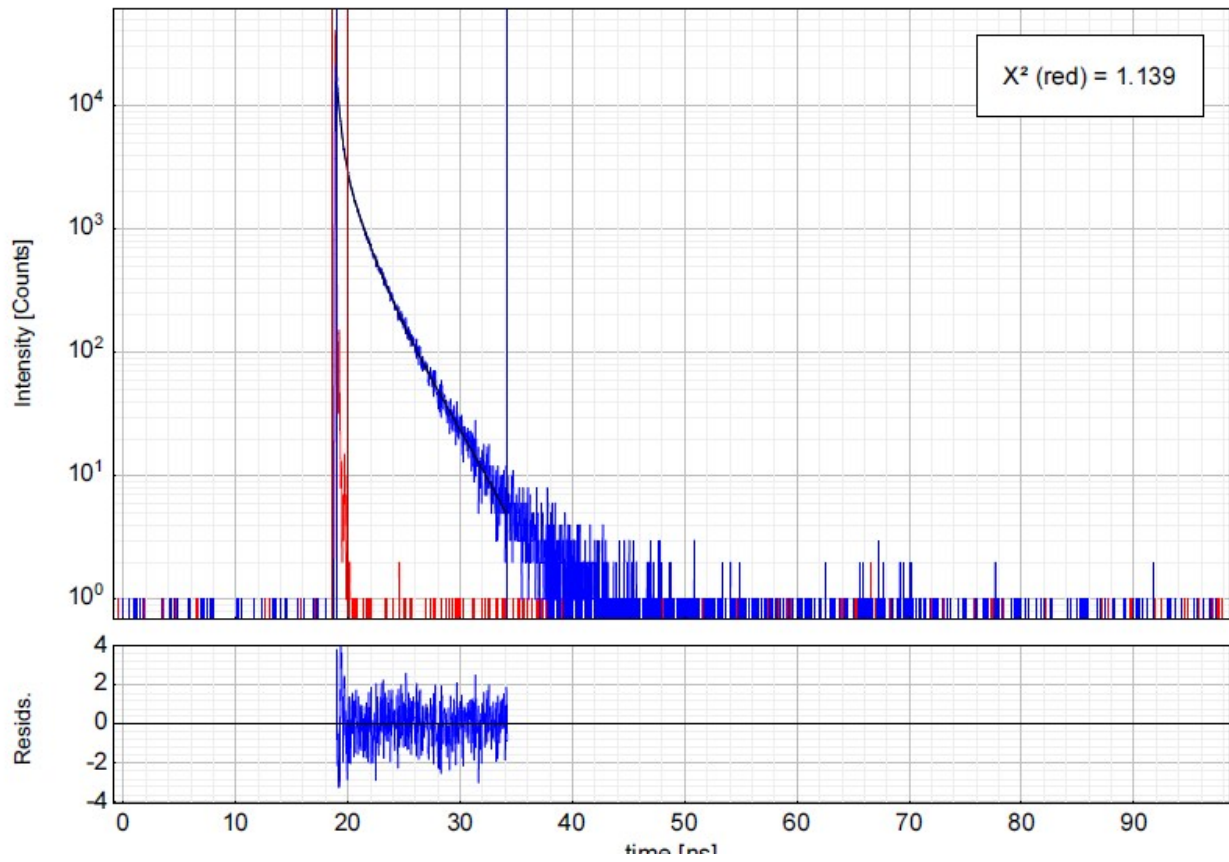


Figure S37. Time-resolved emission decay profile and fit for phosphorescence 12.7 μM at 77 K, pH 7.4 in HEPES Buffer monitored at 407 nm following 325 nm light excitation.

Eu-Coumarin – Eu.L



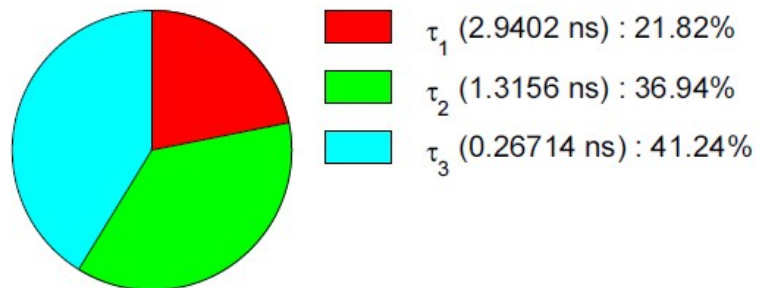
Parameter	Value	Conf. Lower	Conf. Upper	Conf. Estimation
A_1 [Cnts]	977	-153	+153	Fitting
τ_1 [ns]	2.9402	-0.0223	+0.0296	Support Plane
A_2 [Cnts]	3696	-431	+431	Fitting
τ_2 [ns]	1.3156	-0.0094	+0.0128	Support Plane
A_3 [Cnts]	20320	-2330	+2330	Fitting
τ_3 [ns]	0.26714	-0.00096	+0.00159	Support Plane
Bkgr. Dec [Cnts]	-0.96	-8.19	+8.19	Fitting
Bkgr. IRF [Cnts]	-126.3	-89.7	+89.7	Fitting
Shift IRF [ns]	-0.9193	-0.0250	+0.0250	Fitting
A_{Scat} [Cnts]	56000	-208000	+208000	Fitting

Average Lifetime:

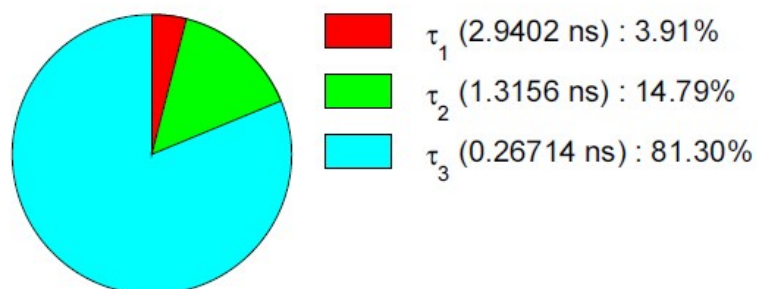
$$\tau_{Av,1} = 1.2378 \text{ ns (intensity weighted)}$$

$$\tau_{Av,2} = 0.5267 \text{ ns (amplitude weighted)}$$

Fractional Intensities of the Positive Decay Components:



Fractional Amplitudes of the Positive Decay Components:



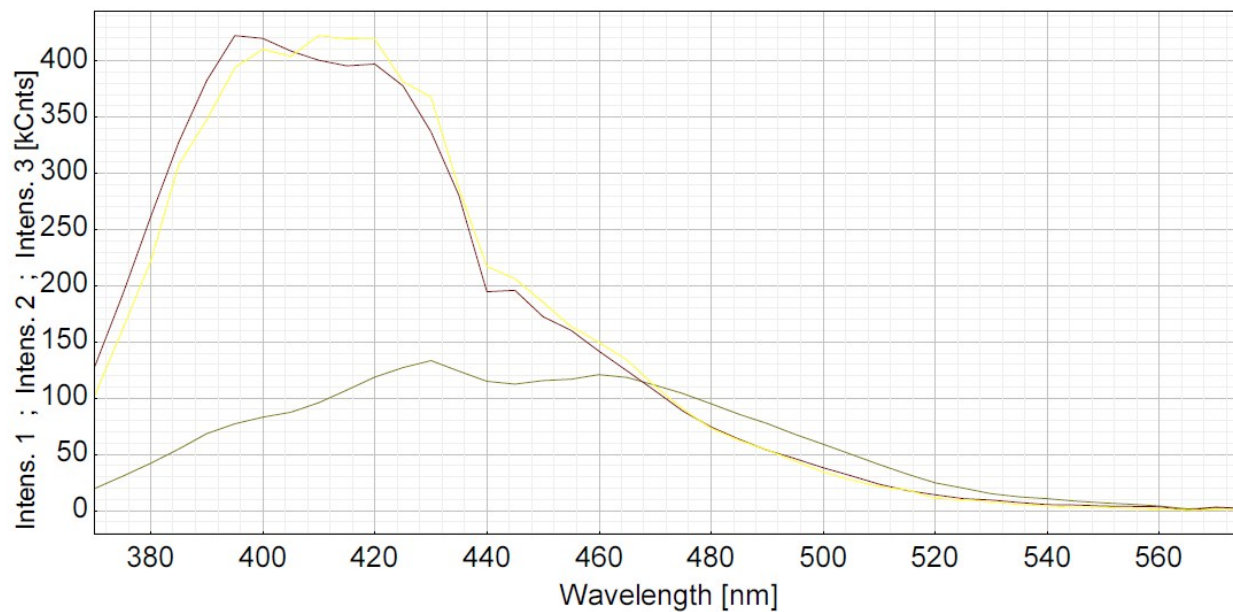
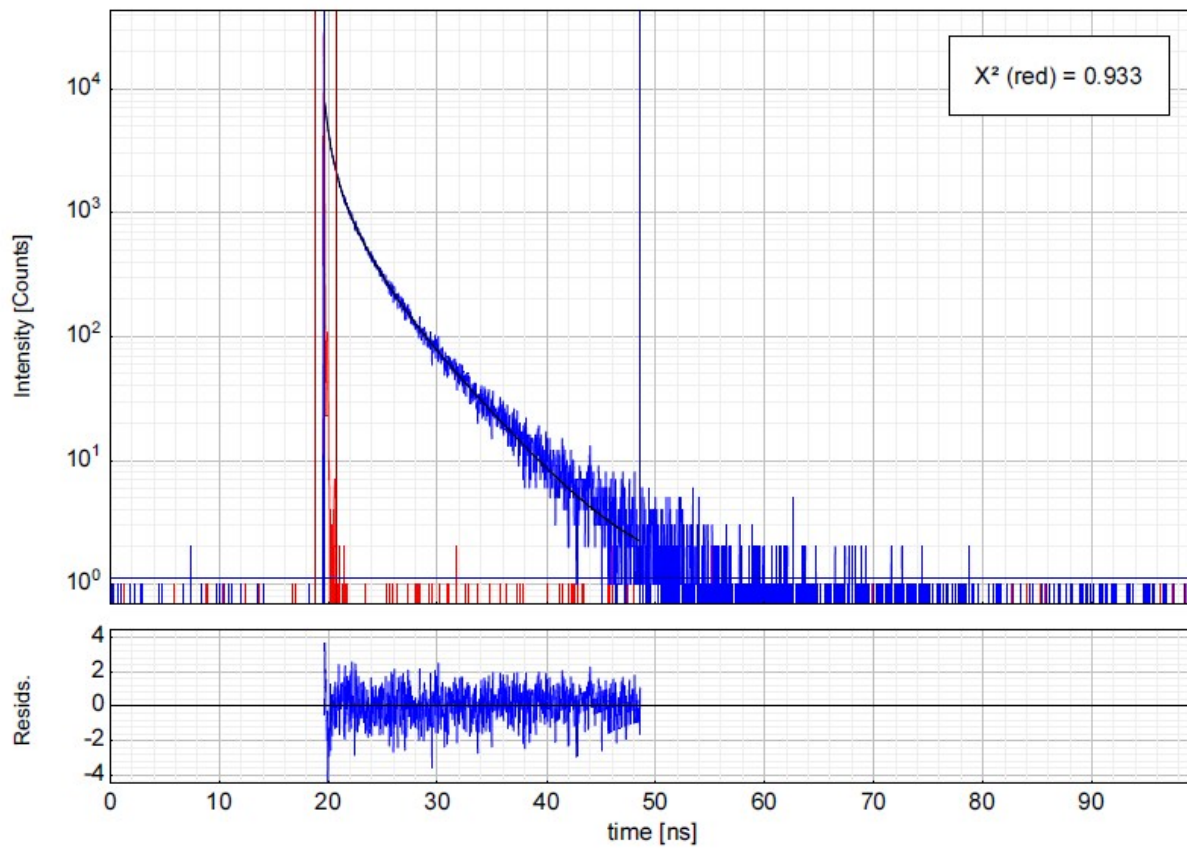


Figure S38. Fluorescence decay profile observed for Coumarin (Eu) in HEPES Buffer pH 7.4. Top, time-resolved emission decay profile. Middle, result of global fit from time resolved emission spectra. Bottom, emission spectra deconvoluted using three lifetime components. The data was fitted to a triexponential decay to determine the associated lifetimes.



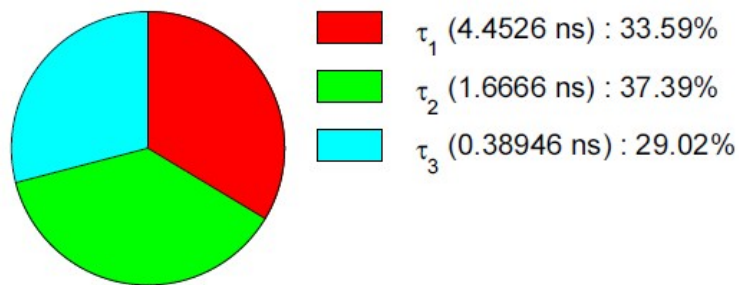
Parameter	Value	Conf. Lower	Conf. Upper	Conf. Estimation
A_1 [Cnts]	668.2	-95.8	+95.8	Fitting
τ_1 [ns]	4.4526	-0.0335	+0.0350	Support Plane
A_2 [Cnts]	1987	-297	+297	Fitting
τ_2 [ns]	1.6666	-0.0104	+0.0102	Support Plane
A_3 [Cnts]	6600	-1020	+1020	Fitting
τ_3 [ns]	0.38946	-0.00291	+0.00284	Support Plane
Bkgr. Dec [Cnts]	1.13	-4.06	+4.06	Fitting
Bkgr. IRF [Cnts]	-117.5	-76.8	+76.8	Fitting
Shift IRF [ns]	1.2172	-0.0155	+0.0155	Fitting
A_{Scat} [Cnts]	-8850	-5790	+5790	Fitting

Average Lifetime:

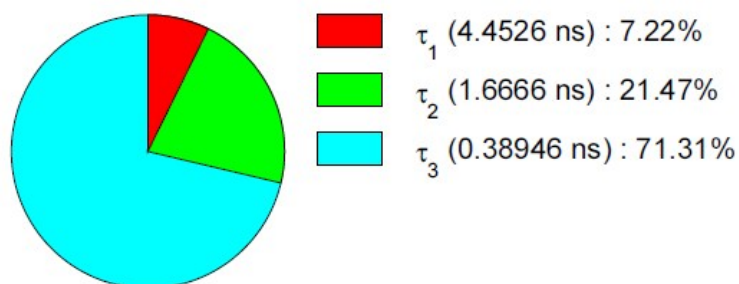
$$\tau_{Av,1} = 2.2318 \text{ ns (intensity weighted)}$$

$$\tau_{Av,2} = 0.9570 \text{ ns (amplitude weighted)}$$

Fractional Intensities of the Positive Decay Components:



Fractional Amplitudes of the Positive Decay Components:



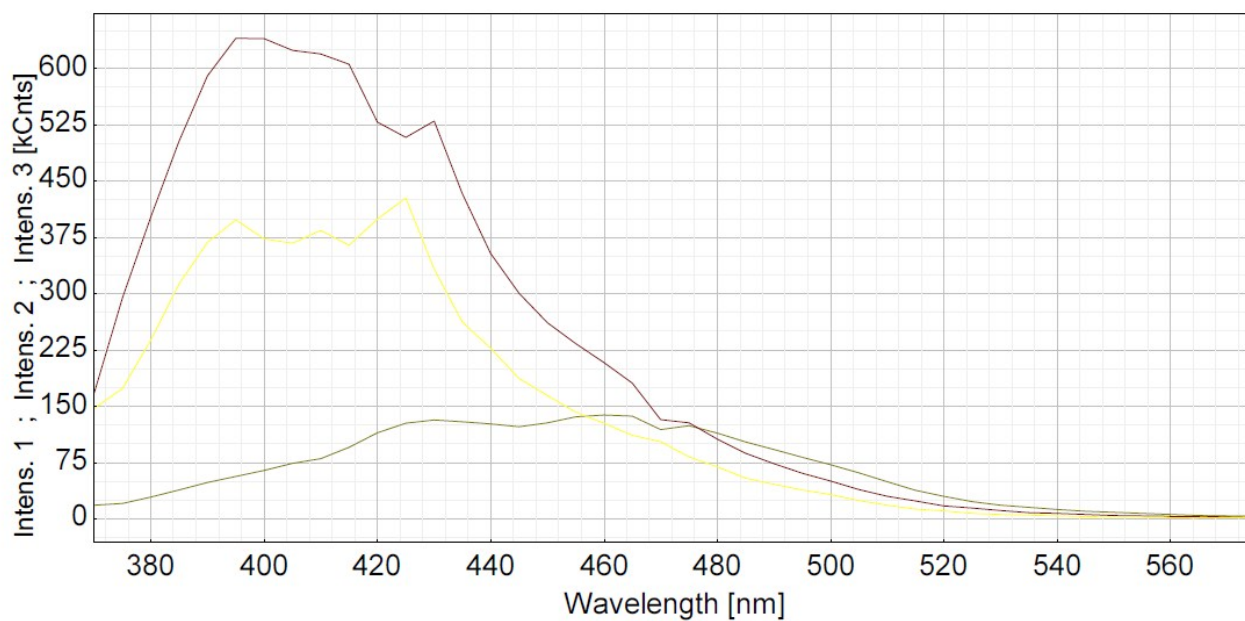


Figure S39. Fluorescence decay profile observed for Coumarin (Eu) in D₂O HEPES Buffer pH 7.4. Top, time-resolved emission decay profile. Middle, result of global fit from time resolved emission spectra. Bottom, emission spectra deconvoluted using three lifetime components. The data was fitted to a triexponential decay to determine the associated lifetimes.

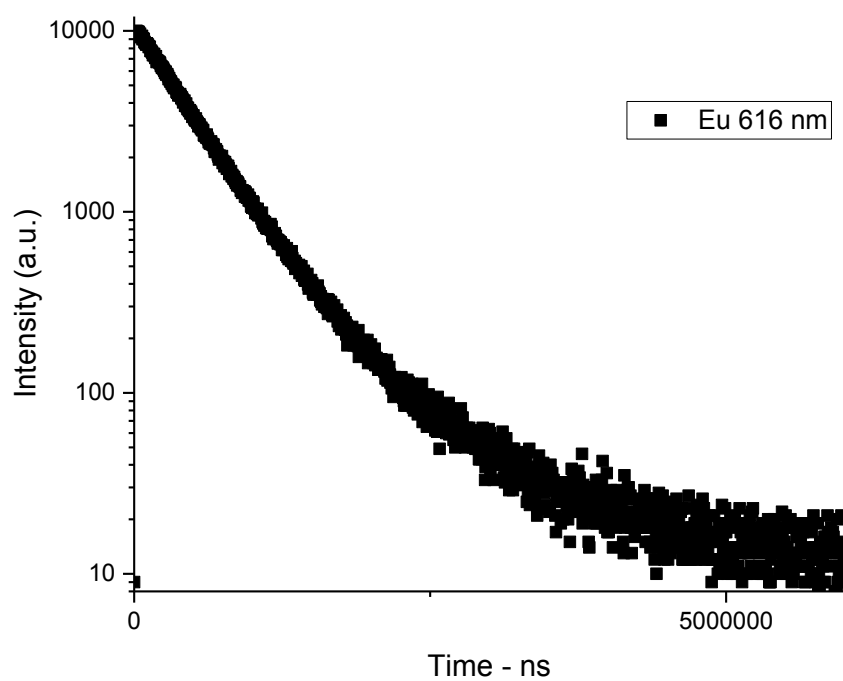
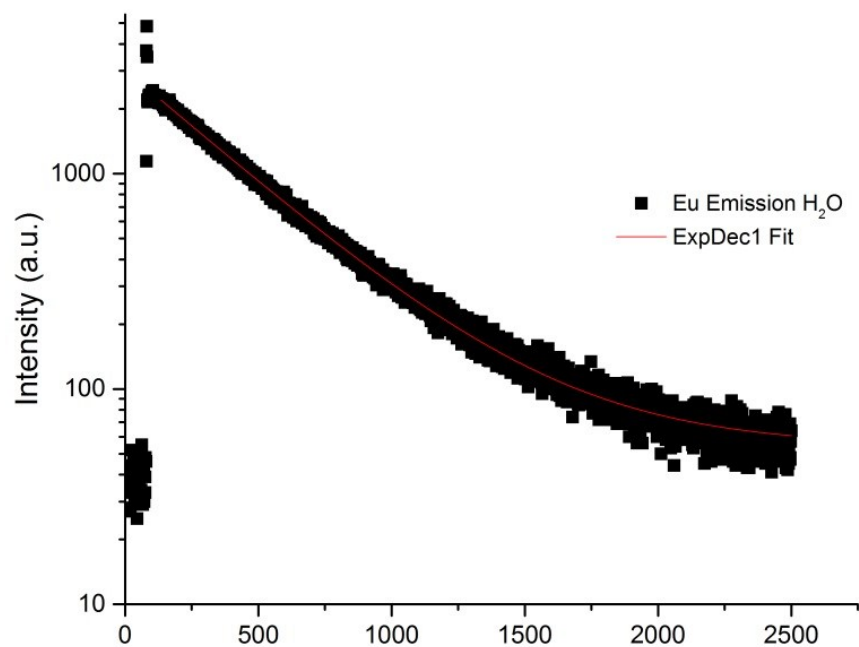


Figure S40. Time-resolved emission decay profile and fit for Eu centred emission 12.7 μ M, pH 7.4 in HEPES Buffer monitored at 616 nm following 325 nm light excitation. Top: First determination. Bottom: Second determination.

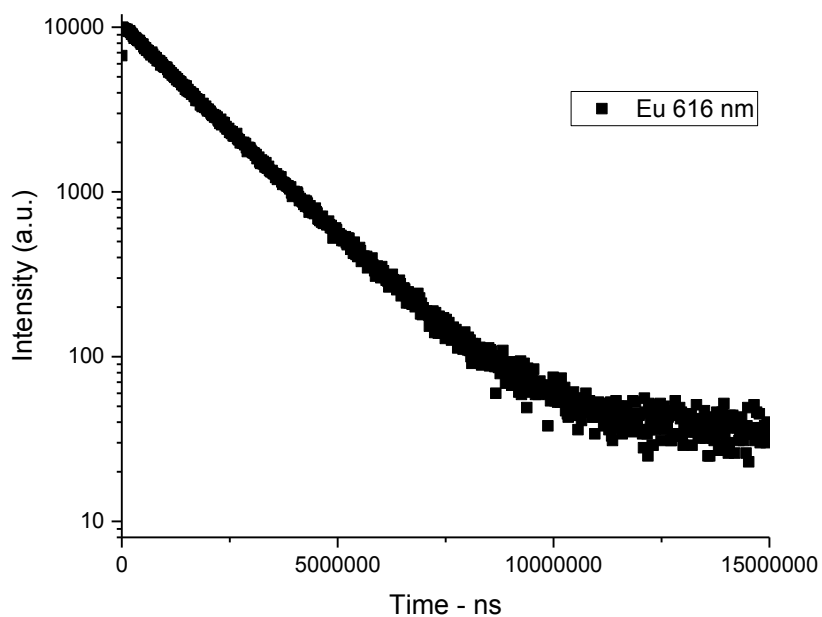
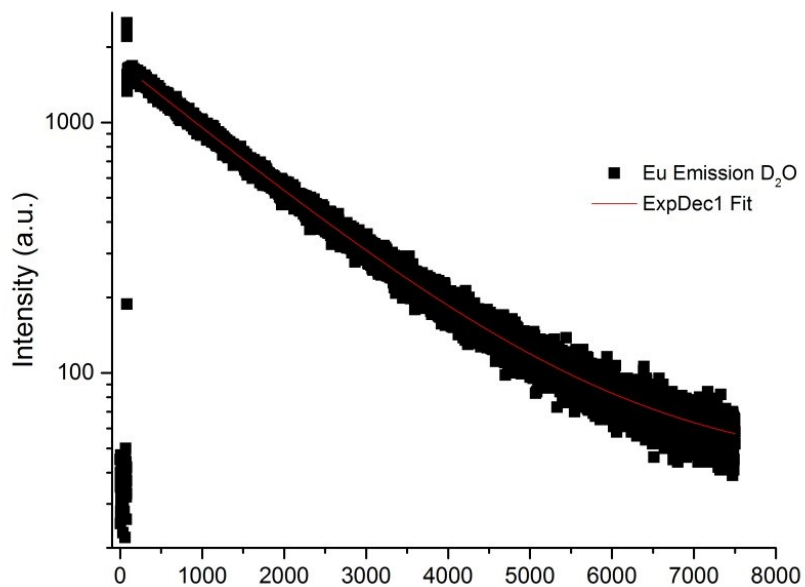


Figure S41. Time-resolved emission decay profile and fit for Eu centred emission 12.7 μM , pH 7.4 in D₂O HEPES Buffer monitored at 616 nm following 325 nm light excitation. Top: First determination. Bottom: Second determination.

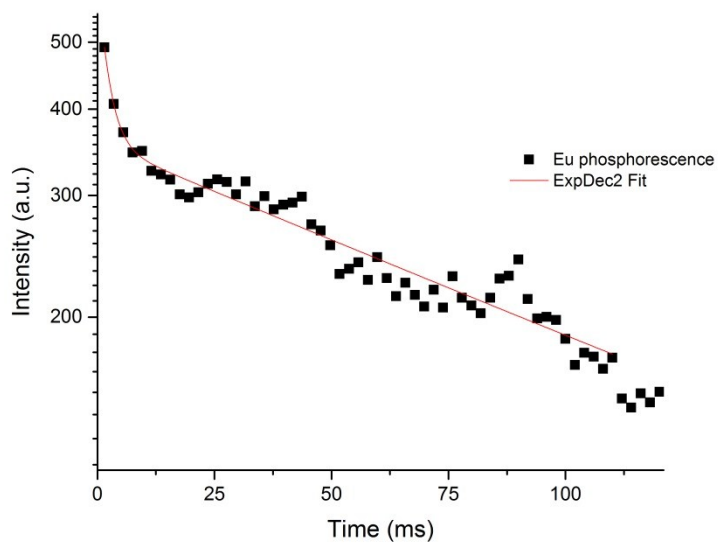
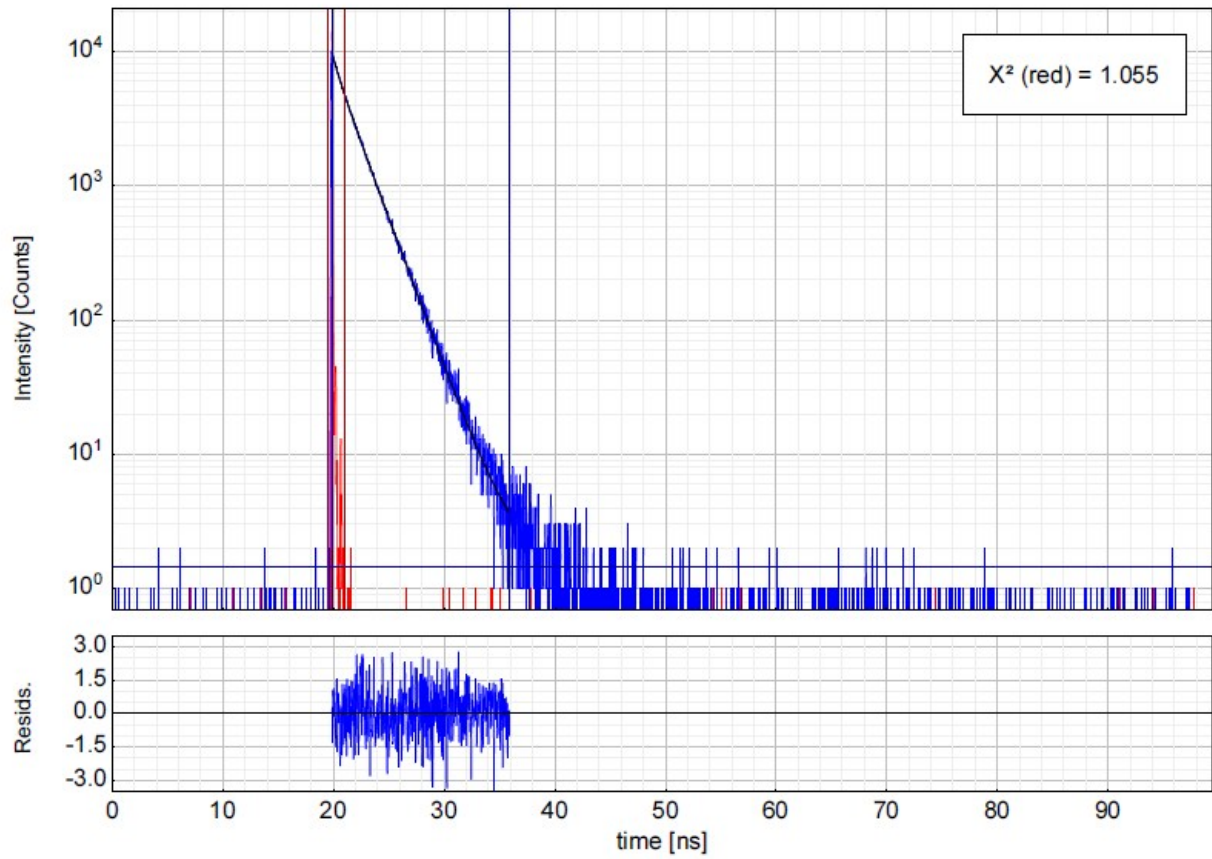


Figure S42. Time-resolved emission decay profile and fit for Eu centred phosphorescence at 77 K, 12.7 μ M, pH 7.4 in HEPES Buffer monitored at 616 nm following 325 nm light excitation.

Gd-Coumarin – Gd.L



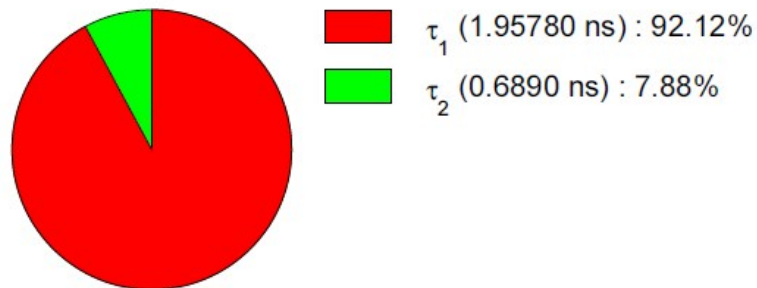
Parameter	Value	Conf. Lower	Conf. Upper	Conf. Estimation
A_1 [Cnts]	8043	-306	+306	Fitting
τ_1 [ns]	1.95780	-0.00305	+0.00623	Support Plane
A_2 [Cnts]	1955	-715	+715	Fitting
τ_2 [ns]	0.6890	-0.0138	+0.0328	Support Plane
Bkgr. Dec [Cnts]	1.44	-6.01	+6.01	Fitting
Bkgr. IRF [Cnts]	-1.47	-23.3	+23.3	Fitting
Shift IRF [ns]	0.3043	-0.0339	+0.0339	Fitting
A_{Scat} [Cnts]	8060	-9920	+9920	Fitting

Average Lifetime:

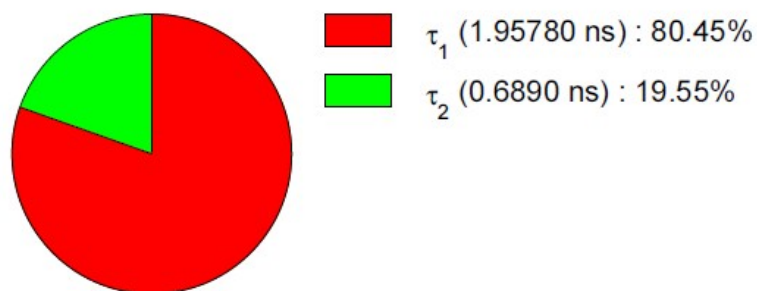
$$\tau_{Av,1} = 1.85782 \text{ ns (intensity weighted)}$$

$$\tau_{Av,2} = 1.70970 \text{ ns (amplitude weighted)}$$

Fractional Intensities of the Positive Decay Components:



Fractional Amplitudes of the Positive Decay Components:



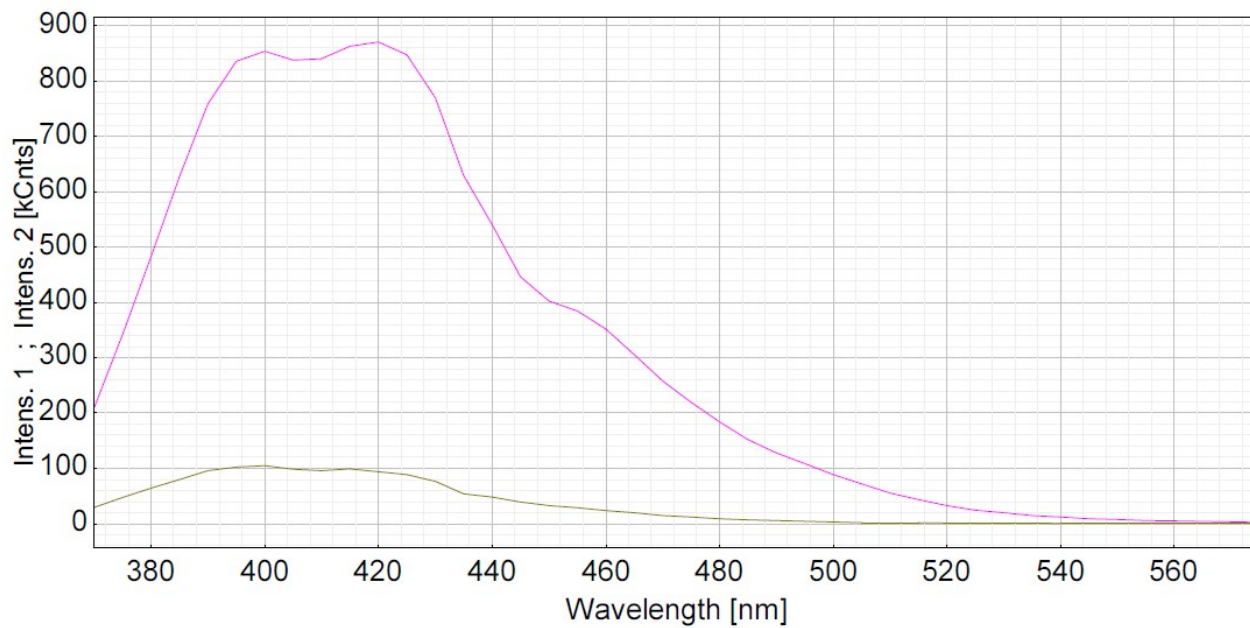
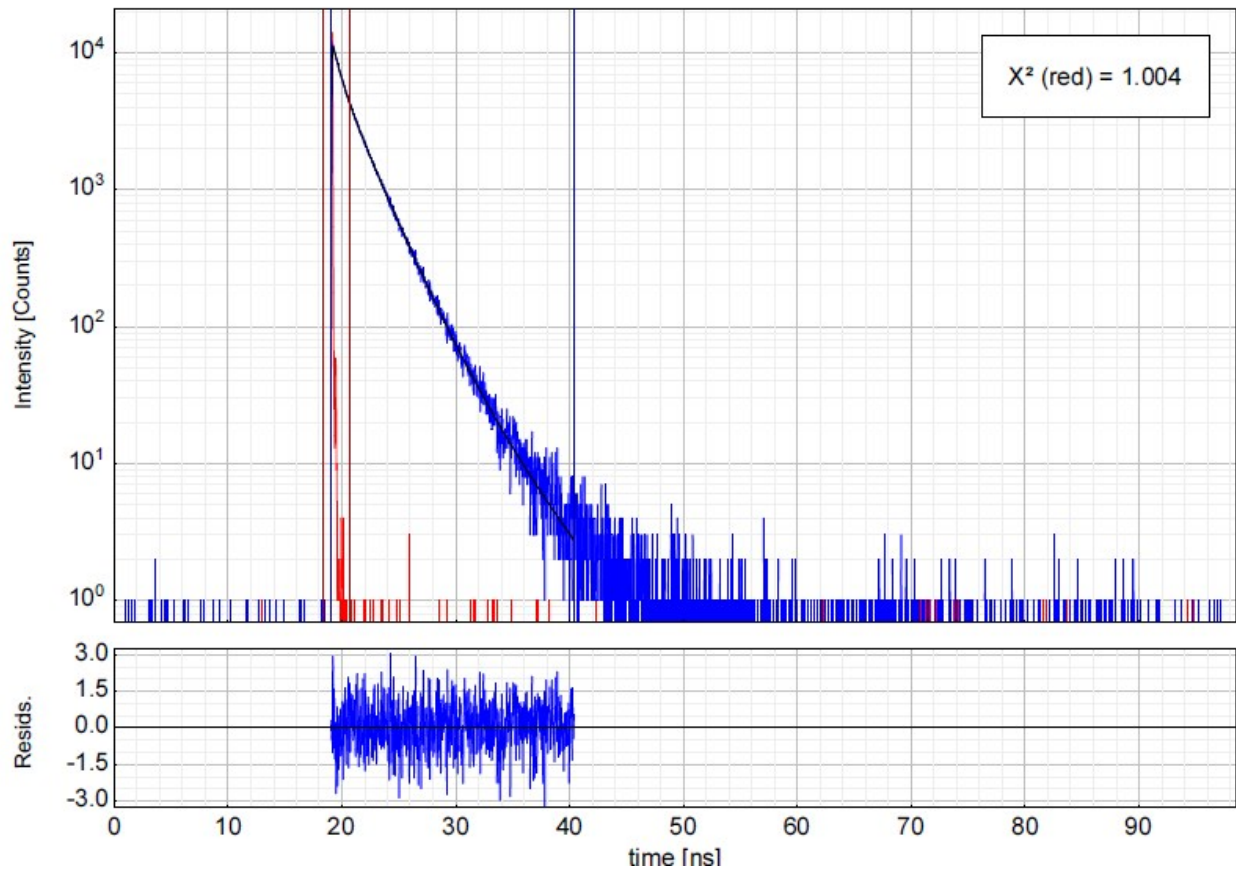


Figure S43. Fluorescence decay profile observed for Coumarin (Gd) in HEPES Buffer pH 7.4. Top, time-resolved emission decay profile. Middle, result of global fit from time resolved emission spectra. Bottom, emission spectra deconvoluted using three lifetime components. The data was fitted to a diexponential decay to determine the associated lifetimes.



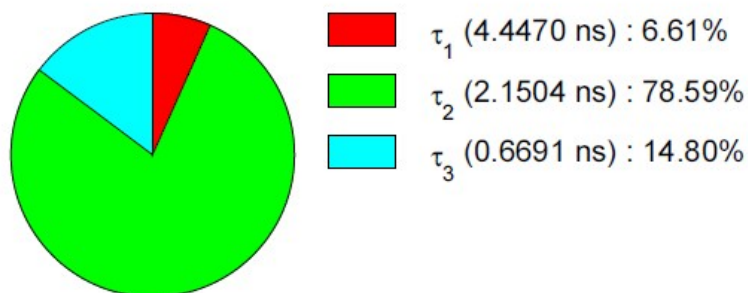
Parameter	Value	Conf. Lower	Conf. Upper	Conf. Estimation
A ₁ [Cnts]	307	-111	+111	Fitting
τ ₁ [ns]	4.4470	-0.0833	+0.0848	Support Plane
A ₂ [Cnts]	7543	-314	+314	Fitting
τ ₂ [ns]	2.1504	-0.0122	+0.0116	Support Plane
A ₃ [Cnts]	4564	-797	+797	Fitting
τ ₃ [ns]	0.6691	-0.0127	+0.0124	Support Plane
Bkgr. Dec [Cnts]	-0.209	-4.79	+4.79	Fitting
Bkgr. IRF [Cnts]	0.428	-11.9	+11.9	Fitting
Shift IRF [ns]	3.08966	-0.00777	+0.00777	Fitting
A _{Scat} [Cnts]	-1700	-4620	+4620	Fitting

Average Lifetime:

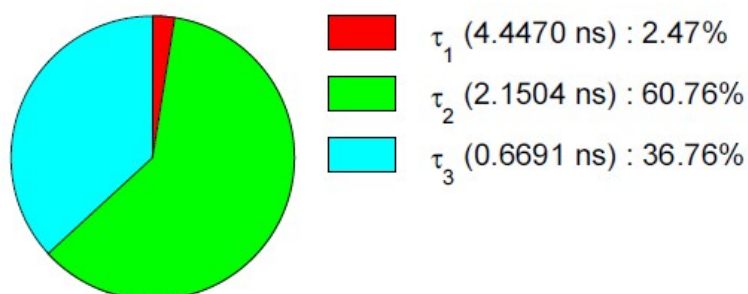
$$\tau_{Av,1} = 2.0831 \text{ ns (intensity weighted)}$$

$$\tau_{Av,2} = 1.6626 \text{ ns (amplitude weighted)}$$

Fractional Intensities of the Positive Decay Components:



Fractional Amplitudes of the Positive Decay Components:



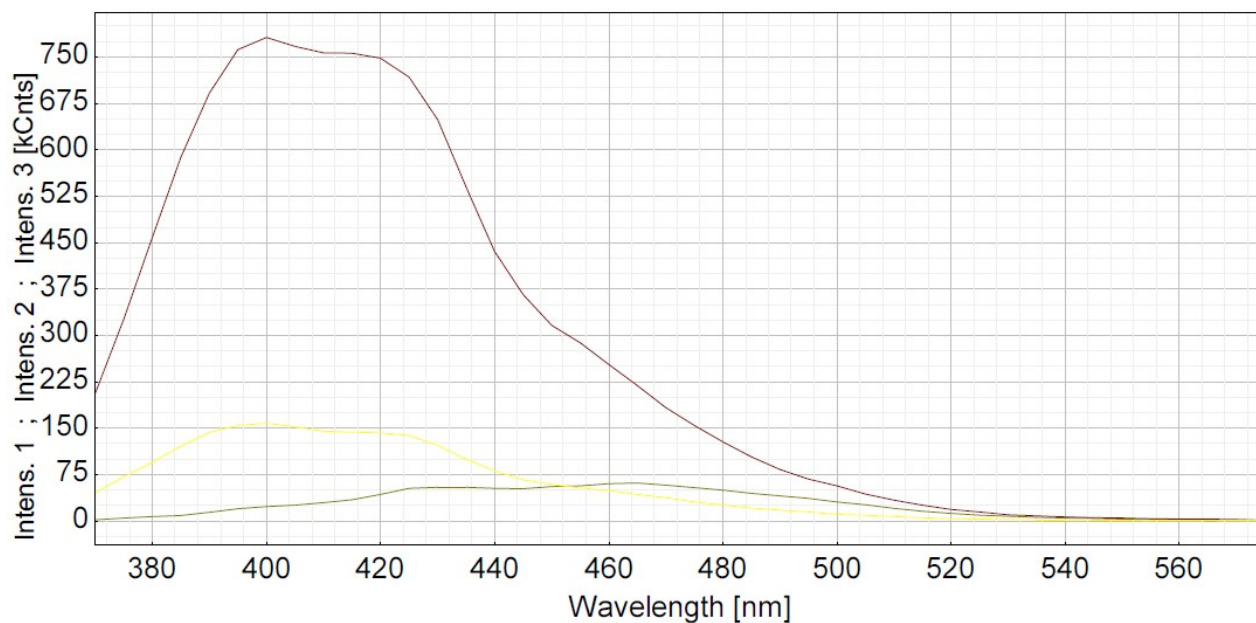


Figure S44. Fluorescence decay profile observed for Coumarin (Gd) in D₂O HEPES Buffer pH 7.4. Top, time-resolved emission decay profile. Middle, result of global fit from time resolved emission spectra. Bottom, emission spectra deconvoluted using three lifetime components. The data was fitted to a triexponential decay to determine the associated lifetimes.

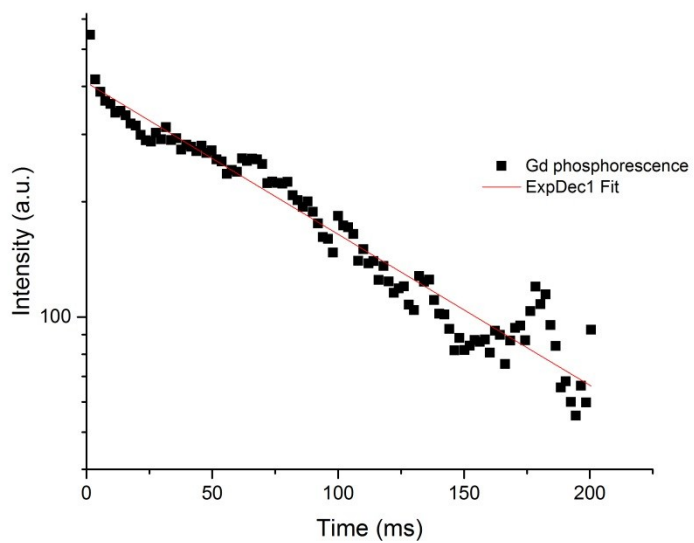
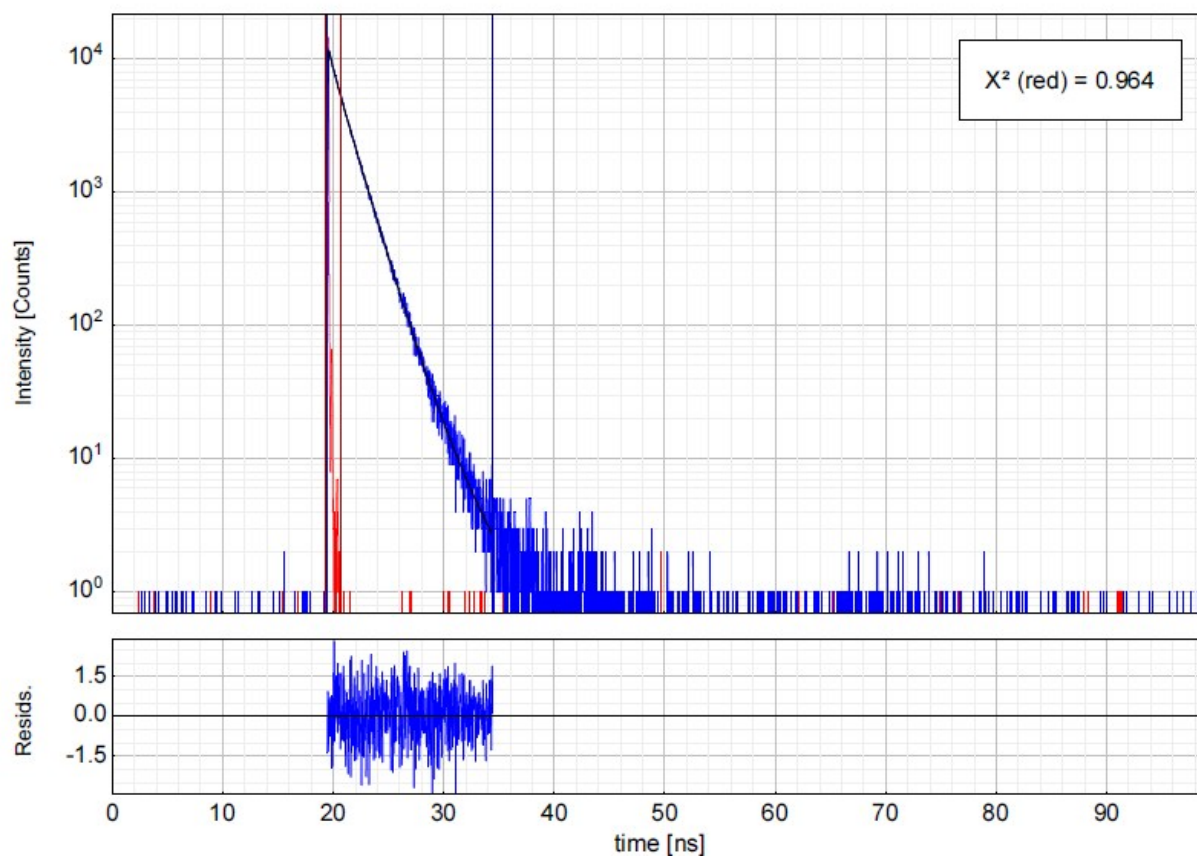


Figure S45. Time-resolved emission decay profile and fit for Eu centred phosphorescence at 77 K, 12.7 μ M, pH 7.4 in HEPES Buffer monitored at 616 nm following 325 nm light excitation.

Tb-Coumarin – Tb.L



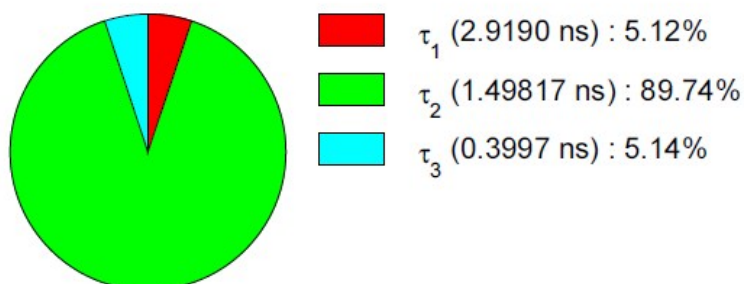
Parameter	Value	Conf. Lower	Conf. Upper	Conf. Estimation
A_1 [Cnts]	302	-134	+134	Fitting
τ_1 [ns]	2.9190	-0.0861	+0.0706	Support Plane
A_2 [Cnts]	10310	-341	+341	Fitting
τ_2 [ns]	1.49817	-0.00900	+0.00651	Support Plane
A_3 [Cnts]	2214	-917	+917	Fitting
τ_3 [ns]	0.3997	-0.0355	+0.0281	Support Plane
Bkgr. Dec [Cnts]	0.280	-4.84	+4.84	Fitting
Bkgr. IRF [Cnts]	-25.8	-23.8	+23.8	Fitting
Shift IRF [ns]	2.36317	-0.00693	+0.00693	Fitting
A_{Scat} [Cnts]	-1880	-3990	+3990	Fitting

Average Lifetime:

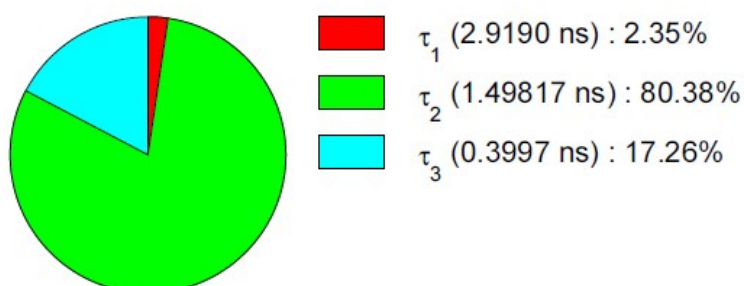
$$\tau_{Av,1} = 1.5145 \text{ ns (intensity weighted)}$$

$$\tau_{Av,2} = 1.3420 \text{ ns (amplitude weighted)}$$

Fractional Intensities of the Positive Decay Components:



Fractional Amplitudes of the Positive Decay Components:



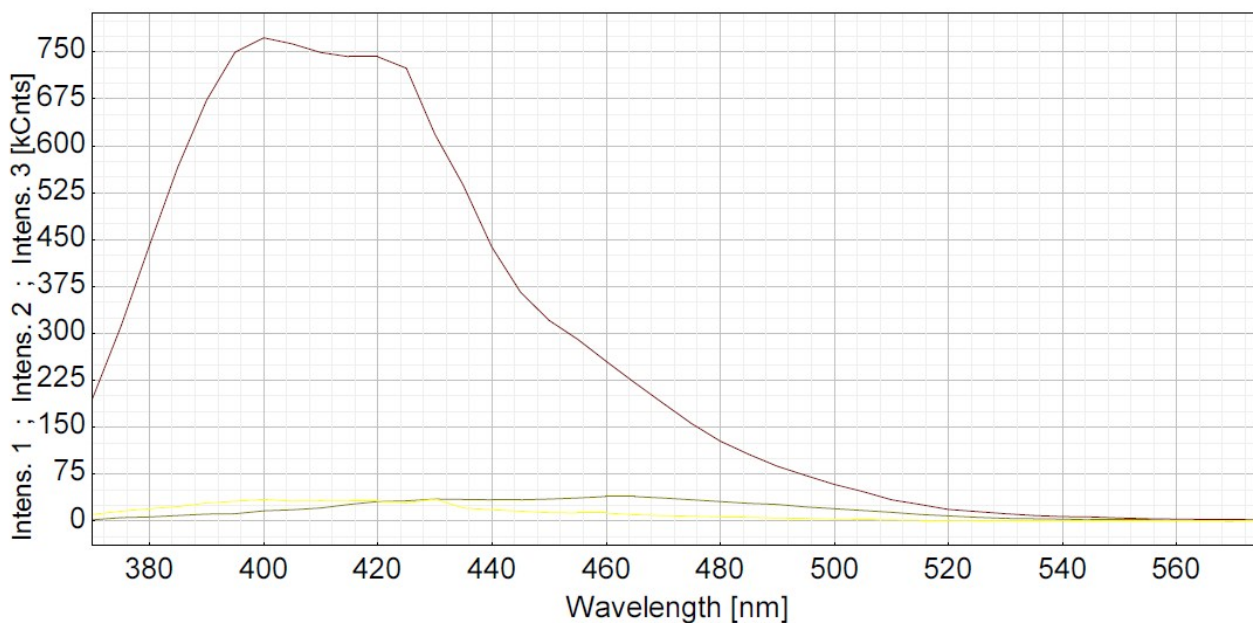
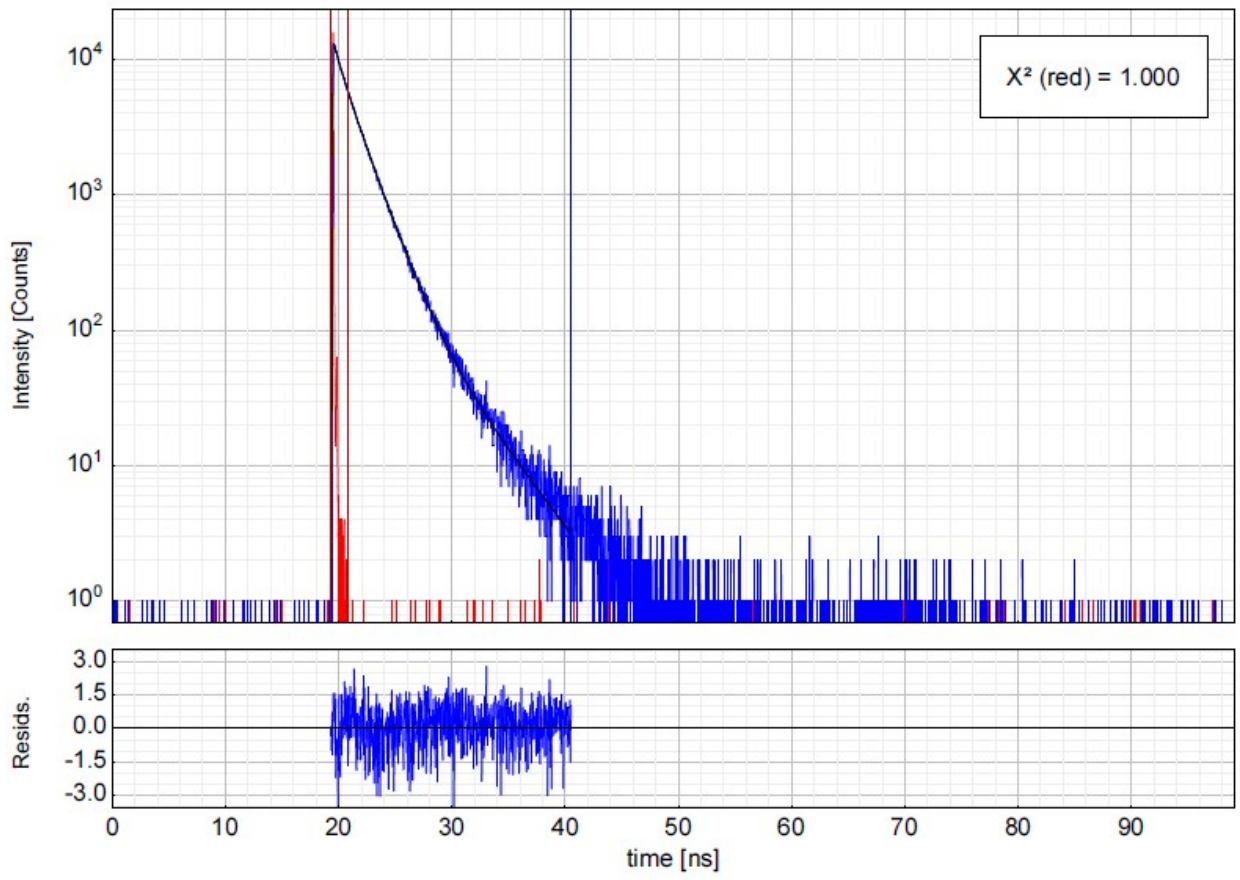


Figure S46. Fluorescence decay profile observed for Coumarin (Tb) in HEPES Buffer pH 7.4. Top, time-resolved emission decay profile. Middle, result of global fit from time resolved emission spectra. Bottom, emission spectra deconvoluted using three lifetime components. The data was fitted to a triexponential decay to determine the associated lifetimes.



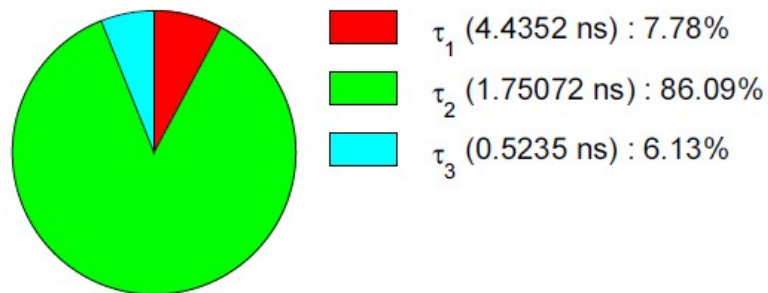
Parameter	Value	Conf. Lower	Conf. Upper	Conf. Estimation
A ₁ [Cnts]	400	-112	+112	Fitting
τ ₁ [ns]	4.4352	-0.0512	+0.0449	Support Plane
A ₂ [Cnts]	11234	-429	+429	Fitting
τ ₂ [ns]	1.75072	-0.00803	+0.00646	Support Plane
A ₃ [Cnts]	2680	-1070	+1070	Fitting
τ ₃ [ns]	0.5235	-0.0282	+0.0228	Support Plane
Bkgr. Dec [Cnts]	-0.428	-5.03	+5.03	Fitting
Bkgr. IRF [Cnts]	-1.52	-16.8	+16.8	Fitting
Shift IRF [ns]	1.54240	-0.00707	+0.00707	Fitting
A _{Scat} [Cnts]	-780	-5370	+5370	Fitting

Average Lifetime:

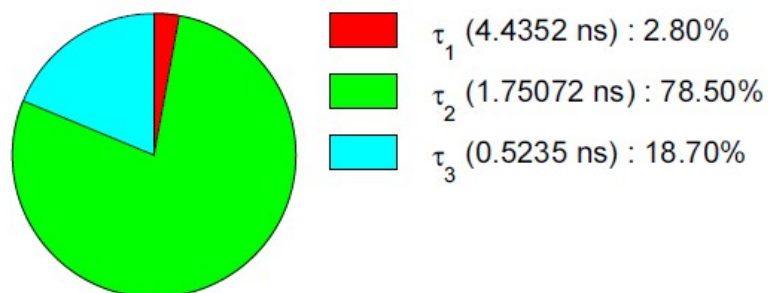
$$\tau_{Av.1} = 1.8842 \text{ ns (intensity weighted)}$$

$$\tau_{Av.2} = 1.5964 \text{ ns (amplitude weighted)}$$

Fractional Intensities of the Positive Decay Components:



Fractional Amplitudes of the Positive Decay Components:



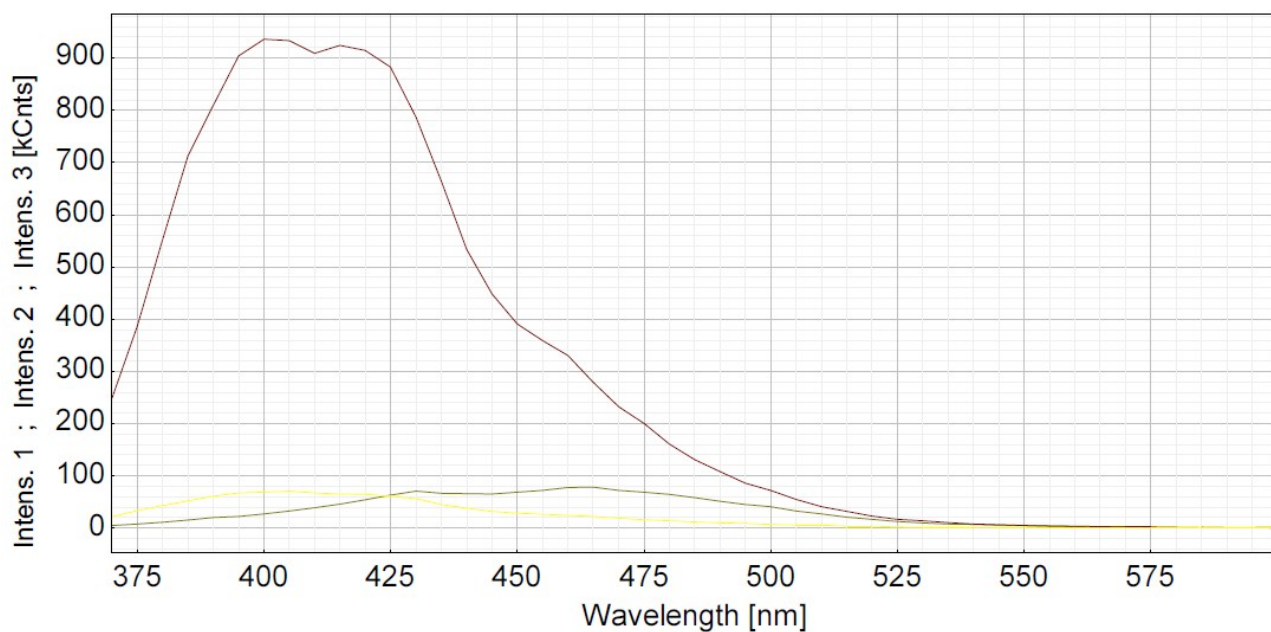


Figure S47. Fluorescence decay profile observed for Coumarin (Tb) in D₂O HEPES Buffer pH 7.4. Top, time-resolved emission decay profile. Middle, result of global fit from time resolved emission spectra. Bottom, emission spectra deconvoluted using three lifetime components. The data was fitted to a triexponential decay to determine the associated lifetimes.

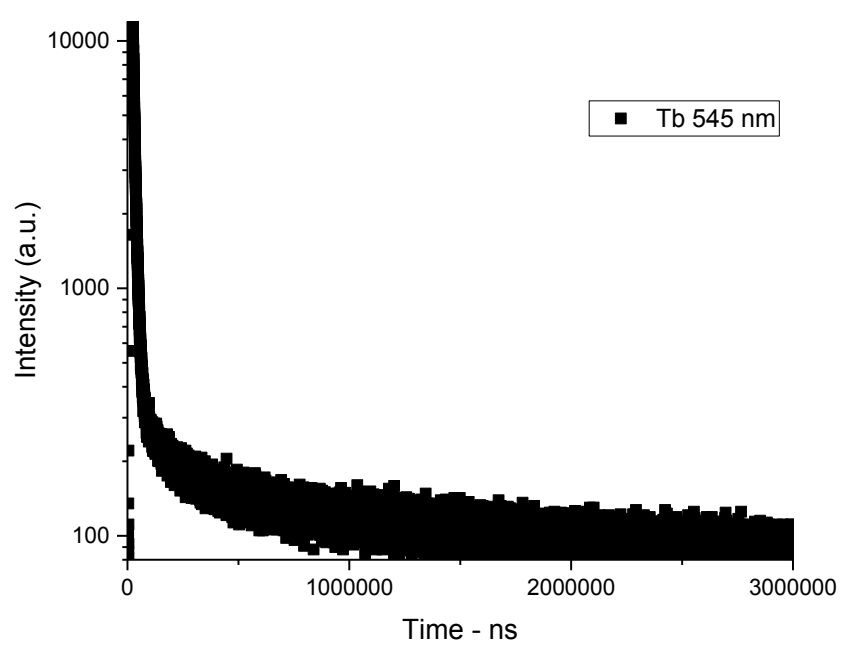
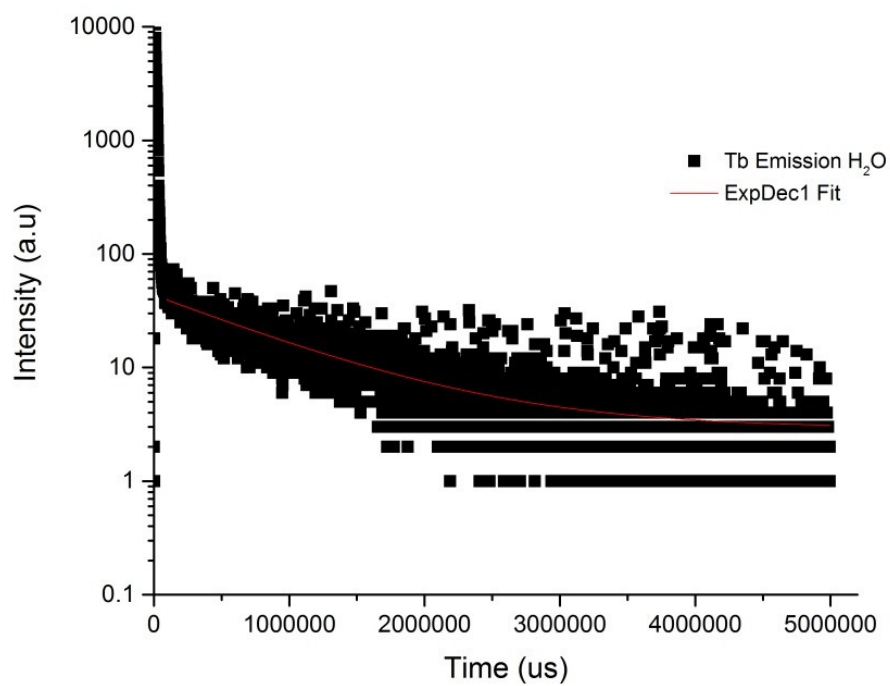


Figure S48. Time-resolved emission decay profile and fit for Tb centred emission 12.7 μ M, pH 7.4 in HEPES Buffer monitored at 545 nm following 325 nm light excitation. Top: First determination. Bottom: Second determination.

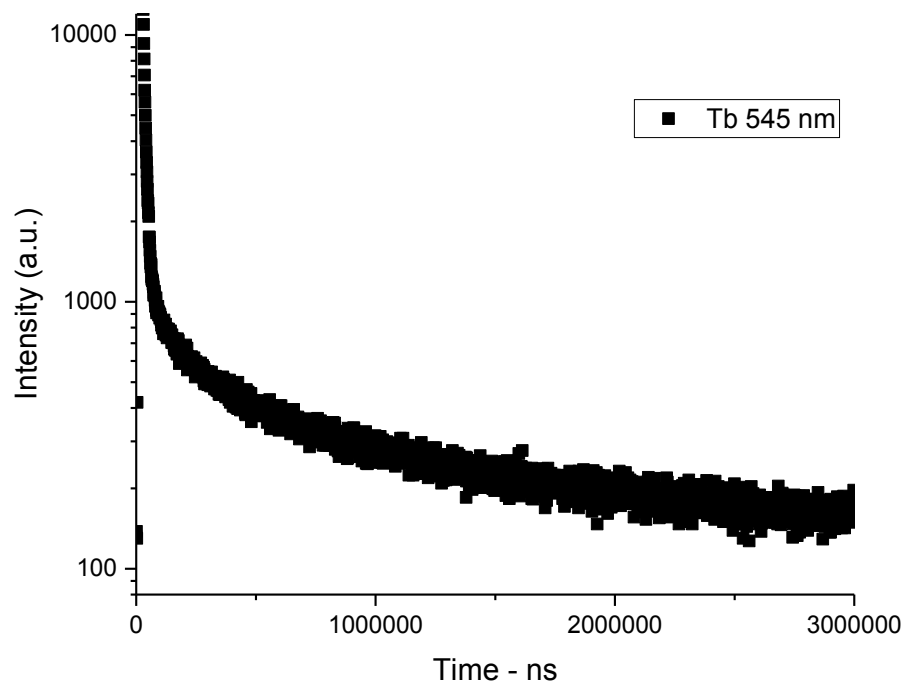
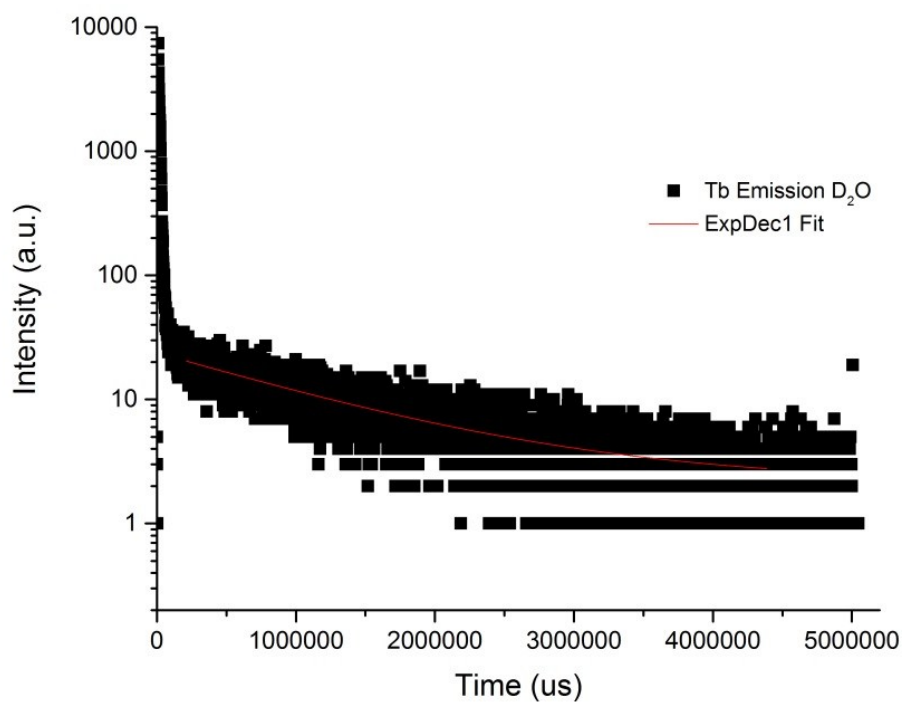


Figure S49. Time-resolved emission decay profile and fit for Tb centred emission 12.7 μM , pH 7.4 in D₂O HEPES Buffer monitored at 545 nm following 325 nm light excitation. Top: First determination. Bottom: Second determination.

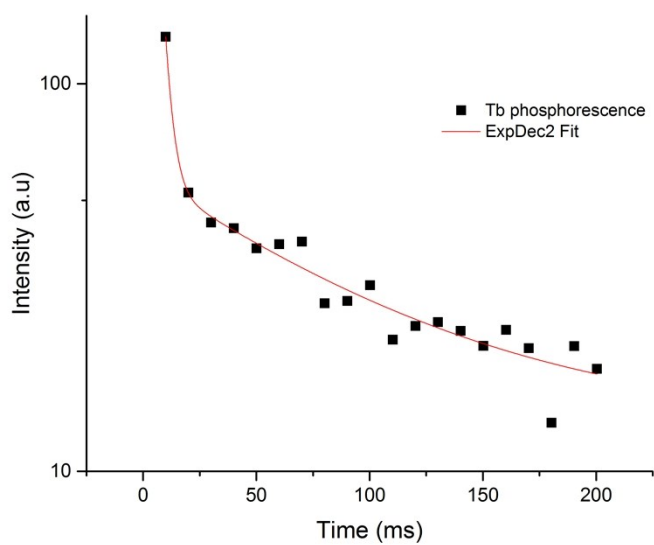
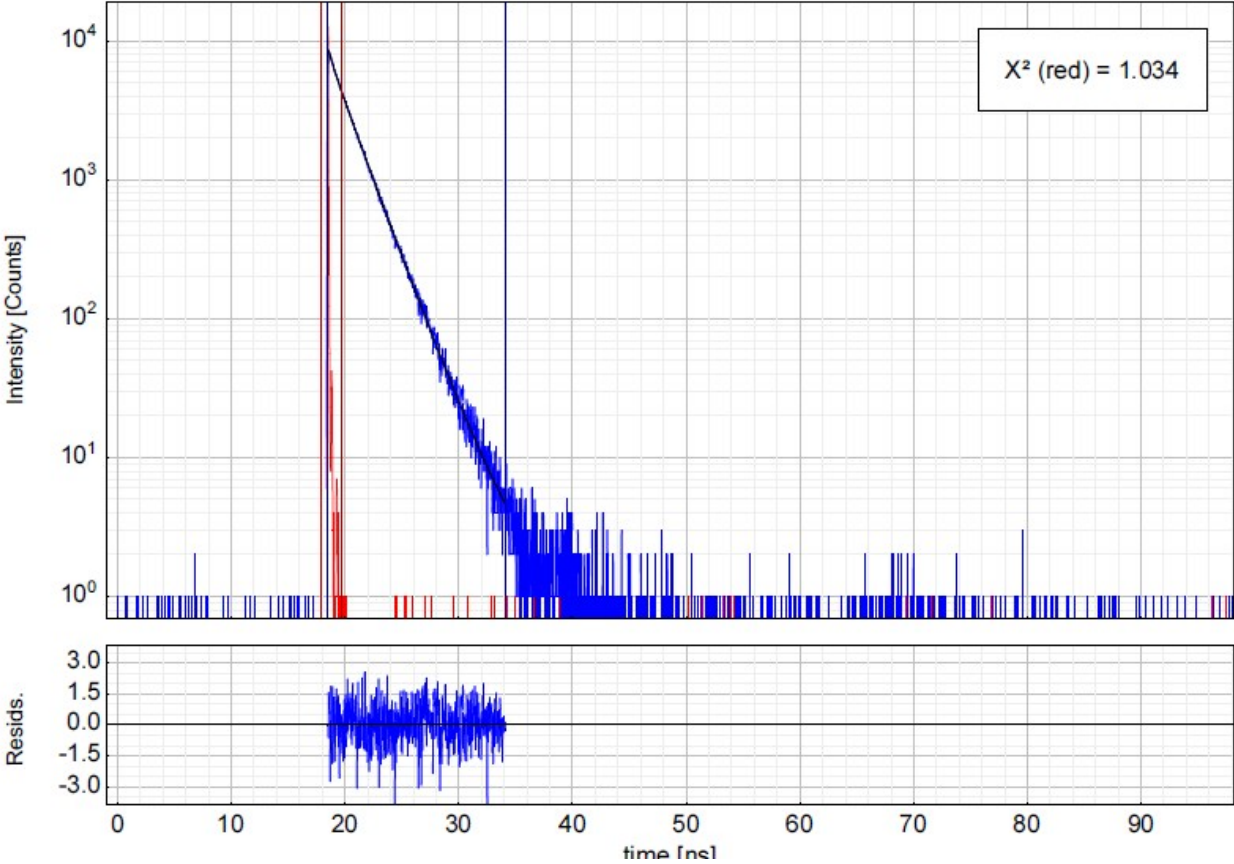


Figure S50. Time-resolved emission decay profile and fit for Tb centred phosphorescence at 77 K, 12.7 μ M, pH 7.4 in HEPES Buffer monitored at 545 nm following 325 nm light excitation.

Y-Coumarin – Y.L



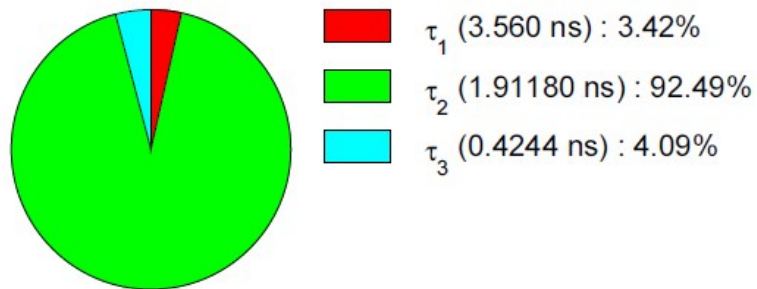
Parameter	Value	Conf. Lower	Conf. Upper	Conf. Estimation
A_1 [Cnts]	151	-115	+115	Fitting
τ_1 [ns]	3.560	-0.157	+0.155	Support Plane
A_2 [Cnts]	7600	-271	+271	Fitting
τ_2 [ns]	1.91180	-0.00977	+0.00831	Support Plane
A_3 [Cnts]	1513	-828	+828	Fitting
τ_3 [ns]	0.4244	-0.0275	+0.0239	Support Plane
Bkgr. Dec [Cnts]	0.494	-6.30	+6.30	Fitting
Bkgr. IRF [Cnts]	-13.6	-18.8	+18.8	Fitting
Shift IRF [ns]	-0.9797	-0.0205	+0.0205	Fitting
A_{Scat} [Cnts]	-433	-5310	+5310	Fitting

Average Lifetime:

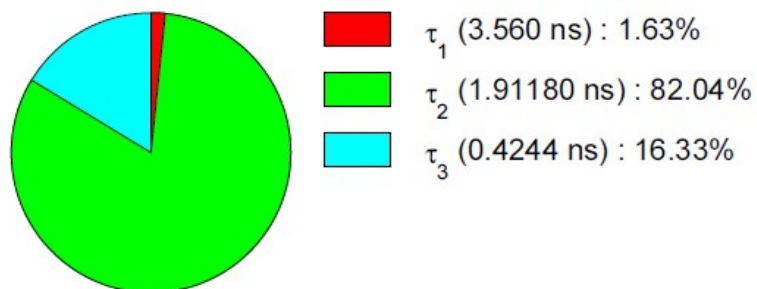
$$\tau_{Av,1} = 1.907 \text{ ns (intensity weighted)}$$

$$\tau_{Av,2} = 1.696 \text{ ns (amplitude weighted)}$$

Fractional Intensities of the Positive Decay Components:



Fractional Amplitudes of the Positive Decay Components:



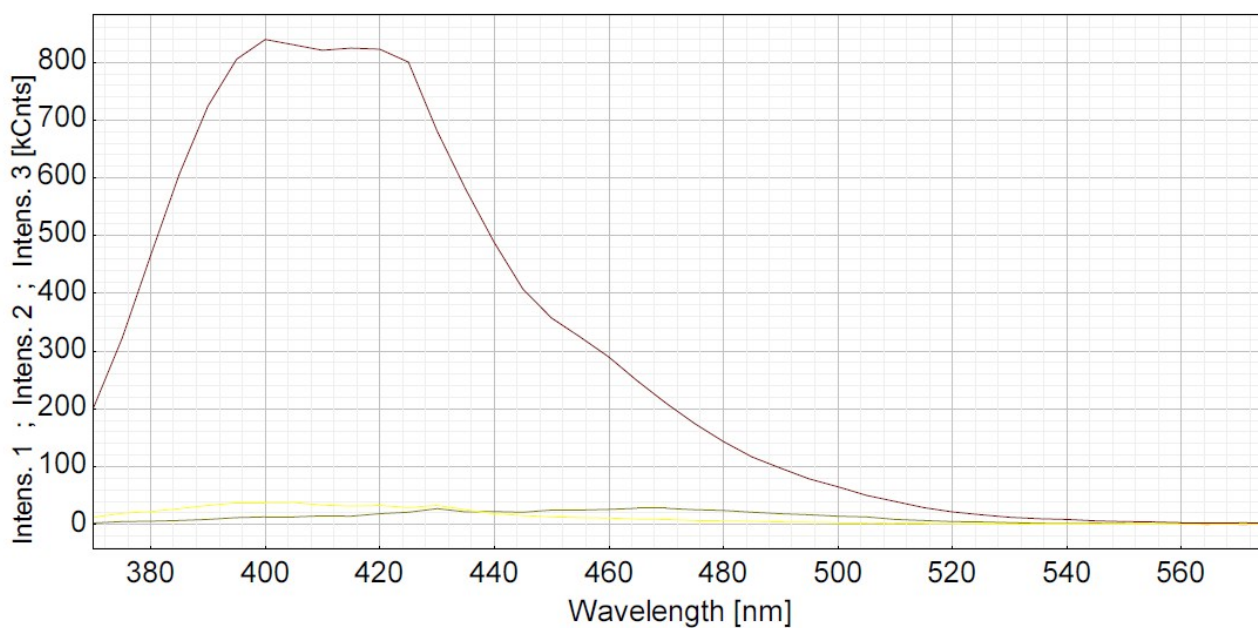
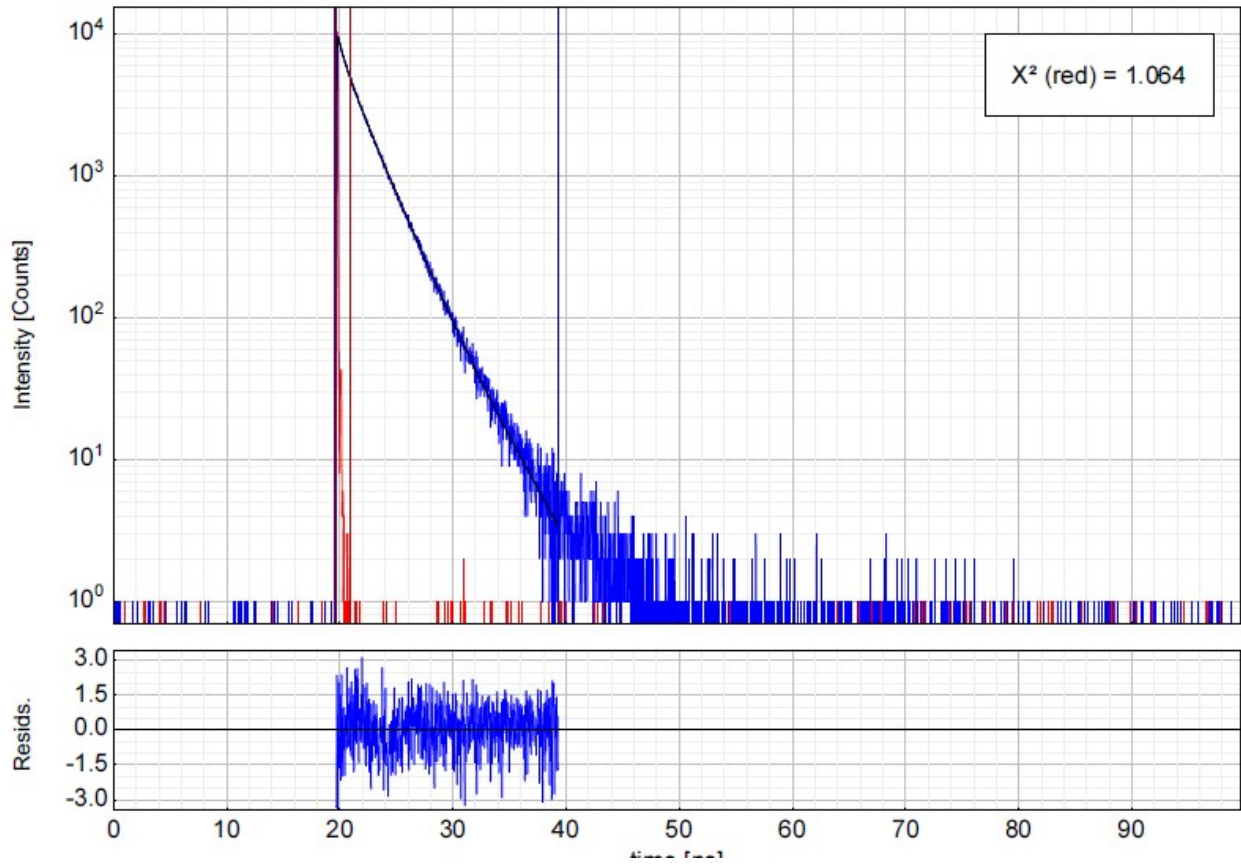


Figure S51. Fluorescence decay profile observed for Coumarin (Y) in HEPES Buffer pH 7.4. Top, time-resolved emission decay profile. Middle, result of global fit from time resolved emission spectra. Bottom, emission spectra deconvoluted using three lifetime components. The data was fitted to a triexponential decay to determine the associated lifetimes.



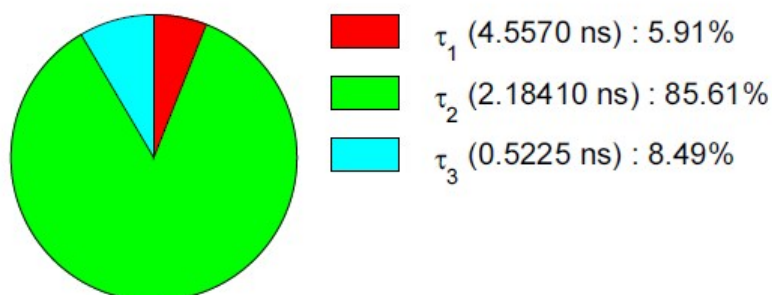
Parameter	Value	Conf. Lower	Conf. Upper	Conf. Estimation
A ₁ [Cnts]	239	-102	+102	Fitting
τ ₁ [ns]	4.5570	-0.0833	+0.0885	Support Plane
A ₂ [Cnts]	7229	-288	+288	Fitting
τ ₂ [ns]	2.18410	-0.00902	+0.01005	Support Plane
A ₃ [Cnts]	2995	-860	+860	Fitting
τ ₃ [ns]	0.5225	-0.0150	+0.0159	Support Plane
Bkgr. Dec [Cnts]	-0.99	-5.67	+5.67	Fitting
Bkgr. IRF [Cnts]	-17.9	-19.2	+19.2	Fitting
Shift IRF [ns]	0.24366	-0.00719	+0.00719	Fitting
A _{Scat} [Cnts]	3270	-4810	+4810	Fitting

Average Lifetime:

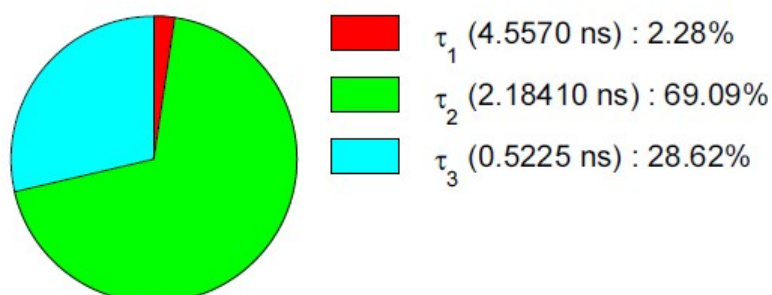
$$\tau_{Av,1} = 2.1832 \text{ ns (intensity weighted)}$$

$$\tau_{Av,2} = 1.7627 \text{ ns (amplitude weighted)}$$

Fractional Intensities of the Positive Decay Components:



Fractional Amplitudes of the Positive Decay Components:



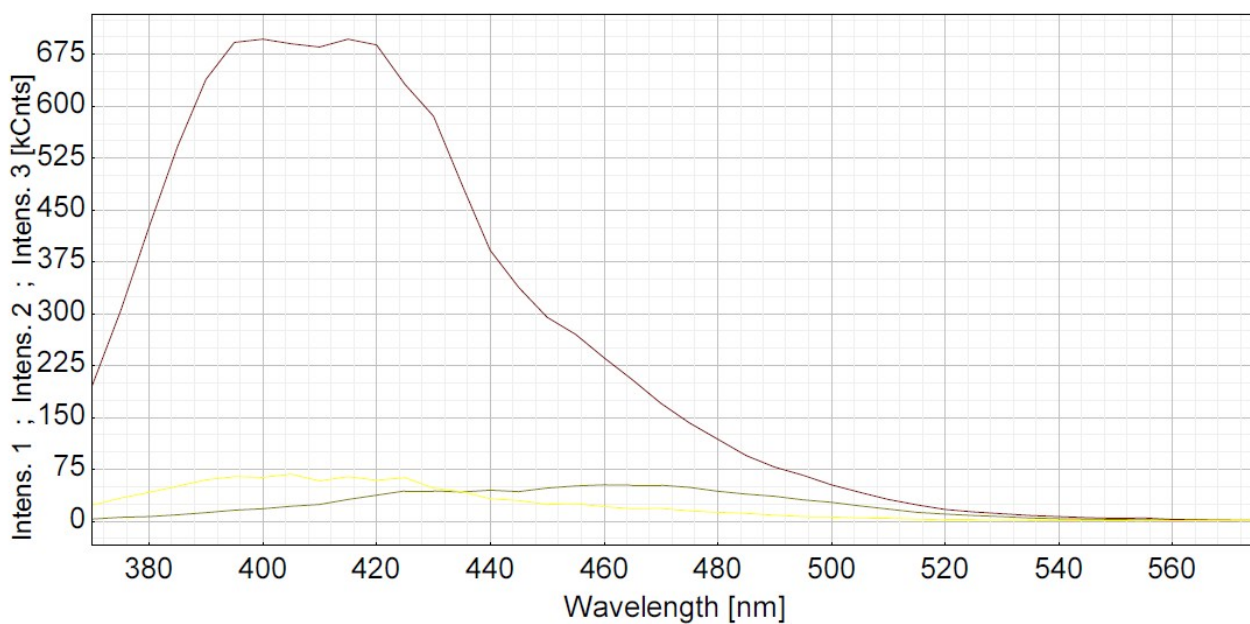


Figure S52. Fluorescence decay profile observed for Coumarin (Y) in D₂O HEPES Buffer pH 7.4. Top, time-resolved emission decay profile. Middle, result of global fit from time resolved emission spectra. Bottom, emission spectra deconvoluted using three lifetime components. The data was fitted to a triexponential decay to determine the associated lifetimes.

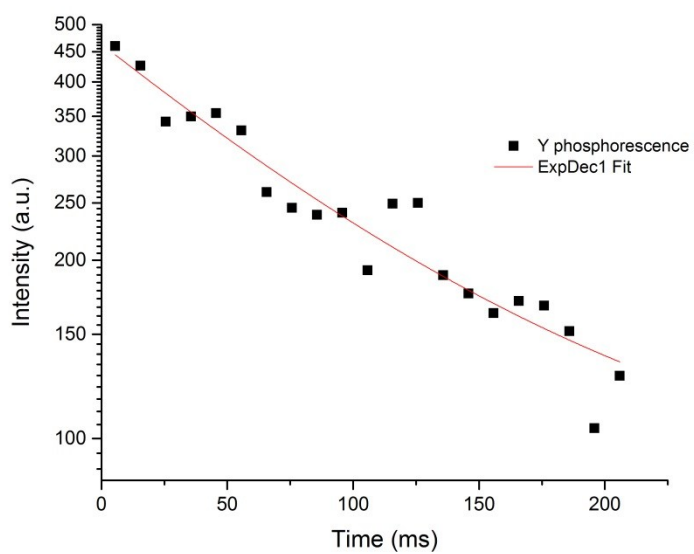


Figure S53. Time-resolved emission decay profile and fit for Coumarin (Y) phosphorescence at 77 K, 12.7 μ M, pH 7.4 in HEPES Buffer monitored at 407 nm following 325 nm light excitation.

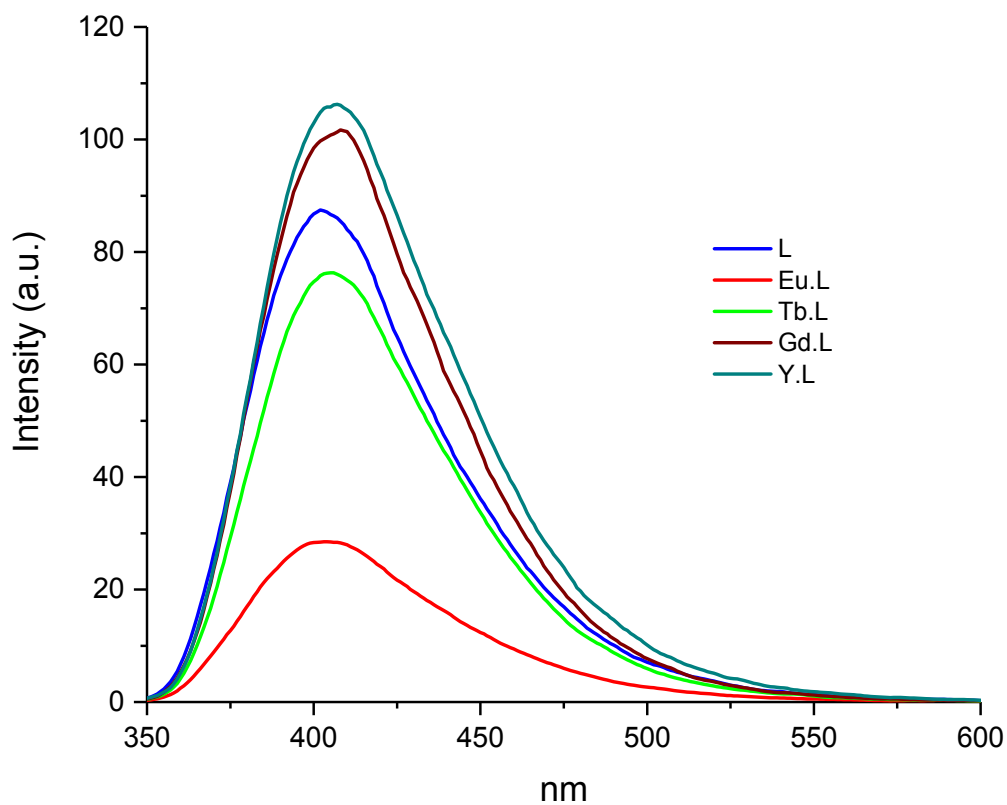
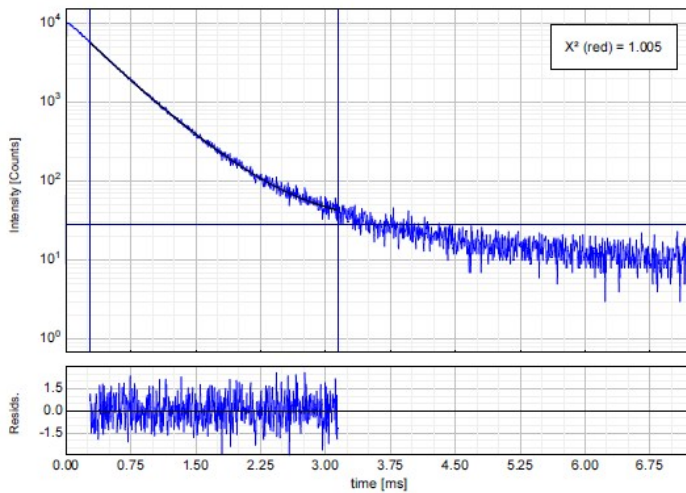


Figure S54. Relative fluorescence intensity of the investigated complexes recorded at identical concentration pH 7.4 in HEPES Buffer and with identical settings.

Main Plot



$$I(t) = \int_{-\infty}^{\infty} \rho(\tau) e^{-\frac{t}{\tau}} d\tau$$

$$\rho(\tau) = \sum_{i=1}^n \frac{A_i}{\pi} \frac{\frac{\Delta_{FWHM_i}}{2}}{(\tau - \tau_i)^2 + \left(\frac{\Delta_{FWHM_i}}{2}\right)^2}$$

PicoQuant FluoFit

2/21/2018

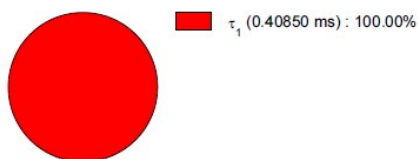


Parameter	Value	Conf. Lower	Conf. Upper	Conf. Estimation
A ₁ [Cnts]	13969.5	-76.0	+76.0	Fitting
τ ₁ [ms]	0.40850	-0.00090	+0.00230	Bootstrap
Δ _{FWHM 1} [ms]	0.16277	-0.00745	+0.00249	Bootstrap
T ₀ [ms]	0.0051006	-0.0000486	+0.0000486	Fitting
Bkgr. Dec. [Cnts]	28.11	-1.94	+1.94	Fitting

Average Lifetime:

τ_{Av,1} = 0.44141 ms (intensity weighted)
 τ_{Av,2} = 0.40850 ms (amplitude weighted)

Fractional Intensities of the Positive Decay Components:



Fractional Amplitudes of the Positive Decay Components:

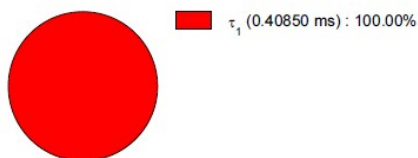
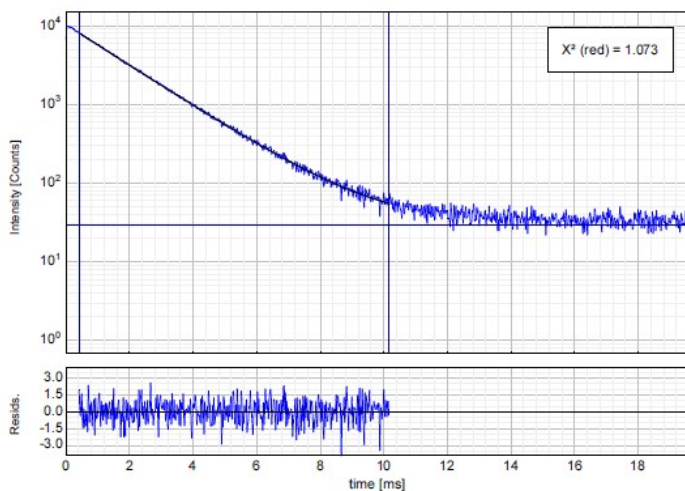


Figure S55. Data analysis using Lorentzian deconvolution of the of time-resolved emission decay profile for Eu centred emission 12.7 μM, pH 7.4 in H₂O HEPES Buffer monitored at 616 nm following 325 nm light excitation..

Main Plot



$$I(t) = \int_0^{\infty} \rho(\tau) e^{-\frac{t}{\tau}} d\tau$$

$$\rho(\tau) = \sum_{i=1}^n \frac{A_i}{\pi} \frac{\frac{\Delta_{FWHM_i}}{2}}{(\tau - \tau_i)^2 + \left(\frac{\Delta_{FWHM_i}}{2}\right)^2}$$

PicoQuant FluoFit

2/21/2018

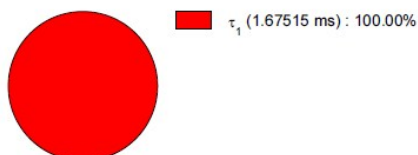


Parameter	Value	Conf. Lower	Conf. Upper	Conf. Estimation
A ₁ [Cnts]	12396.8	-54.6	+54.6	Fitting
τ ₁ [ms]	1.67515	-0.00718	+0.00480	Bootstrap
Δ _{FWHM 1} [ms]	0.171	-0.071	+0.141	Bootstrap
T ₀ [ms]	0.01915	-0.00739	+0.00739	Fitting
Bkgr. Dec. [Cnts]	29.55	-2.45	+2.45	Fitting

Average Lifetime:

τ_{Av,1} = 1.68397 ms (intensity weighted)
 τ_{Av,2} = 1.67515 ms (amplitude weighted)

Fractional Intensities of the Positive Decay Components:



Fractional Amplitudes of the Positive Decay Components:

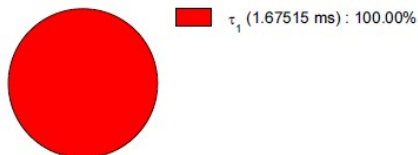
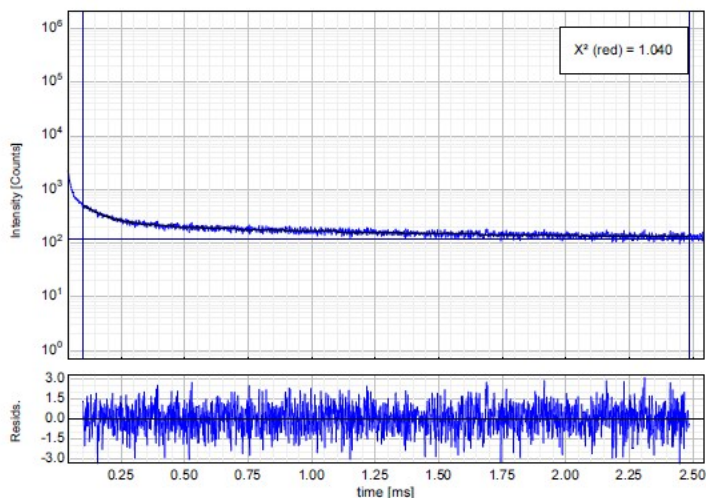


Figure S56. Data analysis of time-resolved emission decay profile and fit for Eu centred emission 12.7 μM, pH 7.4 in D₂O HEPES Buffer monitored at 616 nm following 325 nm light excitation.

Main Plot



$$I(t) = \int_0^{\infty} \rho(\tau) e^{-\frac{t}{\tau}} d\tau$$

$$\rho(\tau) = \sum_{i=1}^n \frac{A_i}{\pi} \frac{\frac{\Delta_{FWHM_i}}{2}}{(\tau - \tau_i)^2 + \left(\frac{\Delta_{FWHM_i}}{2}\right)^2}$$

PicoQuant FluoFit

2/21/2018

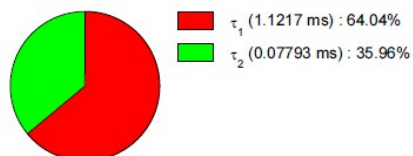


Parameter	Value	Conf. Lower	Conf. Upper	Conf. Estimation
A ₁ [Cnts]	145.86	-6.30	+6.30	Fitting
τ ₁ [ms]	1.1217	-0.0560	+0.0502	Bootstrap
Δ _{FWHM 1} [ms]	0.191	-0.190	+0.0346	Bootstrap
A ₂ [Cnts]	1179	-103	+103	Fitting
τ ₂ [ms]	0.07793	-0.00381	+0.00381	Fitting
Δ _{FWHM 2} [ms]	0.0287	-0.0255	+0.0255	Fitting
T ₀ [ms]	0.006394	-0.000602	+0.000602	Fitting
Bkgr. Dec. [Cnts]	117.80	-2.07	+2.07	Fitting

Average Lifetime:

τ_{Av,1} = 0.7588 ms (intensity weighted)
 τ_{Av,2} = 0.1928 ms (amplitude weighted)

Fractional Intensities of the Positive Decay Components:



Fractional Amplitudes of the Positive Decay Components:

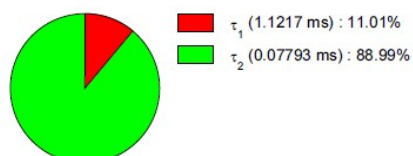
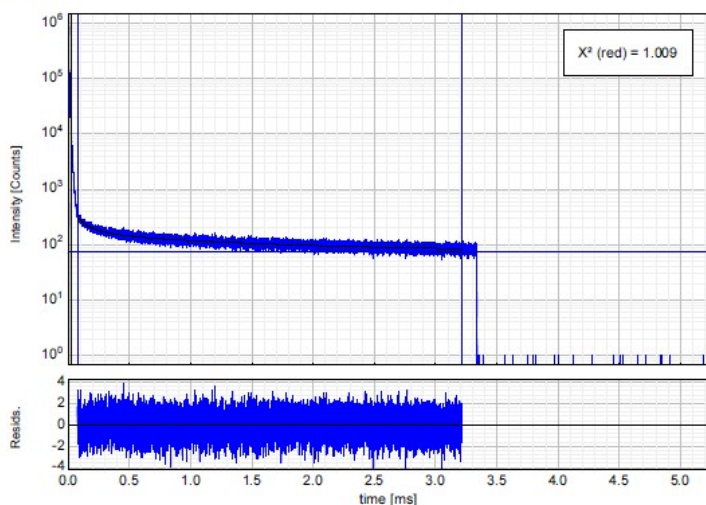


Figure S57. Data analysis of time-resolved emission decay profile and fit for Tb centred emission 12.7 μM, pH 7.4 in H₂O HEPES Buffer monitored at 545 nm following 325 nm light excitation.

Main Plot



$$I(t) = \int_{-\infty}^{\infty} \rho(\tau) e^{-\frac{t}{\tau}} d\tau$$

$$\rho(\tau) = \sum_{i=1}^n \frac{A_i}{\pi} \frac{\frac{\Delta_{FWHM_i}}{2}}{(\tau - \tau_i)^2 + \left(\frac{\Delta_{FWHM_i}}{2}\right)^2}$$

PicoQuant FluoFit

2/21/2018

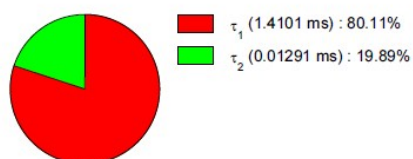


Parameter	Value	Conf. Lower	Conf. Upper	Conf. Estimation
A ₁ [Cnts]	100.99	-4.91	+4.91	Fitting
τ ₁ [ms]	1.4101	-0.00258	+0.0732	Bootstrap
Δ _{FWHM 1} [ms]	0.001051	-0.000051	+0.001452	Bootstrap
A ₂ [Cnts]	848	-104	+104	Fitting
τ ₂ [ms]	0.01291	-0.00853	+0.00853	Fitting
Δ _{FWHM 2} [ms]	0.1288	-0.0165	+0.0165	Fitting
T ₀ [ms]	0.0294	-0.0452	+0.0452	Fitting
Bkgr. Dec [Cnts]	75.60	-1.66	+1.66	Fitting

Average Lifetime:

τ_{Av,1} = 1.1547 ms (intensity weighted)
 τ_{Av,2} = 0.3082 ms (amplitude weighted)

Fractional Intensities of the Positive Decay Components:



Fractional Amplitudes of the Positive Decay Components:

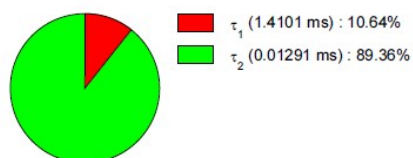


Figure S58. Data analysis of time-resolved emission decay profile and fit for Tb centred emission 12.7 μM, pH 7.4 in D₂O HEPES Buffer monitored at 545 nm following 325 nm light excitation.